LIQUID PHASE METHANATION. MONTHLY PROGRESS REPORT, MAY--NOVEMBER 1972

CHEM SYSTEMS, INC

1972

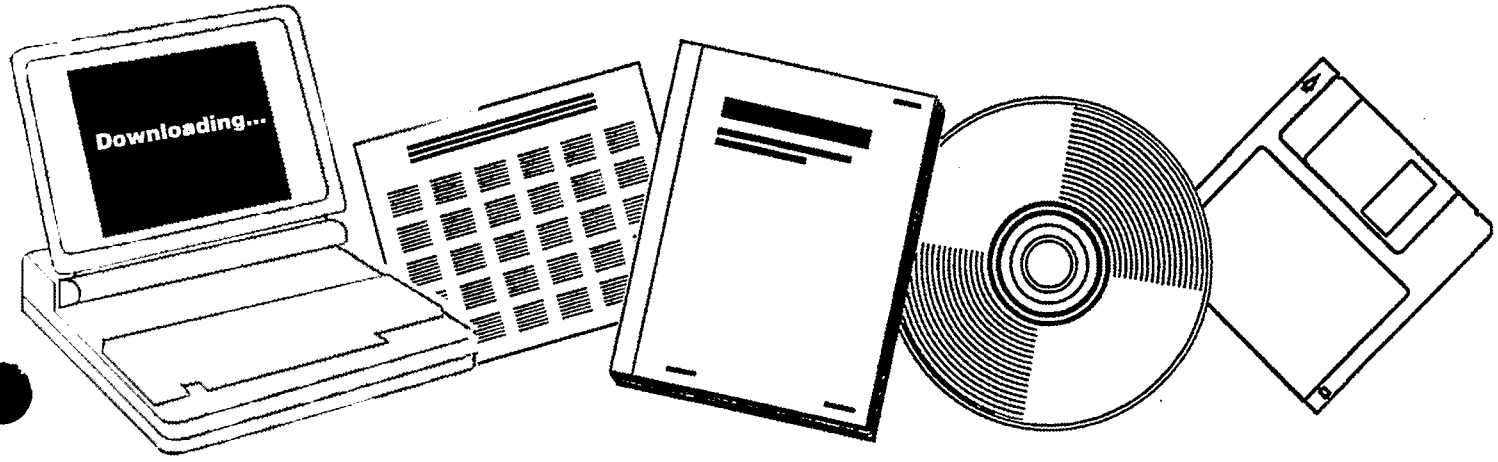

U.S. Department of Commerce
National Technical Information Service

One Source. One Search. One Solution.

NTIS

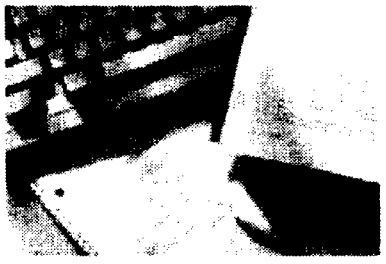

Providing Permanent, Easy Access to U.S. Government Information

National Technical Information Service is the nation's largest repository and disseminator of government-initiated scientific, technical, engineering, and related business information. The NTIS collection includes almost 3,000,000 information products in a variety of formats: electronic download, online access, CD-ROM, magnetic tape, diskette, multimedia, microfiche and paper.

Search the NTIS Database from 1990 forward

NTIS has upgraded its bibliographic database system and has made all entries since 1990 searchable on **www.ntis.gov.** You now have access to information on more than 600,000 government research information products from this web site.

Link to Full Text Documents at Government Web Sites

Because many Government agencies have their most recent reports available on their own web site, we have added links directly to these reports. When available, you will see a link on the right side of the bibliographic screen.

Download Publications (1997 - Present)

NTIS can now provides the full text of reports as downloadable PDF files. This means that when an agency stops maintaining a report on the web, NTIS will offer a downloadable version. There is a nominal fee for each download for most publications.

For more information visit our website:

www.ntis.gov

U.S. DEPARTMENT OF COMMERCE
Technology Administration
National Technical Information Service
Springfield, VA 22161

FE--1505-T-1

LIQUID PHASE METHANATION

Monthly Progress Reports for the
Period May - November 1972

Chem Systems, Inc.
Research Center
275 Hudson Street
Hackensack, N. J. 07601

Prepared for

Office of Coal Research
U. S. Department of the Interior
and
American Gas Association

OCR Contract No. 14-32-0001-1505

FE--1505-T-1

CONTENTS

CSI-MPR--1

Chem Systems Inc.

LIQUID PHASE METHANATION

Progress Report No. 1

Thermal Stability Study

Prepared By Chem Systems Inc.

For The American Gas Association

June 1, 1972

TABLE OF CONTENTS

LIST OF TABLES

LIST OF FIGURES

Experimental Fluid Properties as a Function of Temperature

Engineering Properties

I SUMMARY

During the period prior to May 25, a variety of heat transfer fluids proposed for the Liquid Phase Methanation Project were examined for thermal stability up to temperatures of 650°F. Five of these fluids performed satisfactorily.

1. Dow Corning 550 - Phenyl Methyl Silicone
2. Dowtherm A - Diphenyl-Diphenyl Ether Eutectic
3. Dowtherm G - Di- and Tri-Aryl Ether Mixture
4. 1,2,4-Trimethyl Benzene
5. Hitec - $NaNO_3$ - KNO_3

The paraffinic oil (Sun 21 Heat Transfer Oil) suffered measurable degradation but it should not be discarded at this time. It should be noted that the data provided by the manufacturers indicate that it is thermally stable at 600°F. Moreover, the degradation losses at 650°F are not sufficient to render its use uneconomical but it remains a questionable candidate.

Polyethylene glycols and ethers proved thermally unstable.

In summary, aromatic hydrocarbons are preferable to paraffinics and non-hydrocarbon heat transfer fluids such as salt and silicones appear satisfactory.

II INTRODUCTION

The proposed methanation process involves a cocurrent liquid phase which serves as a sink for the heat evolved by the methanation reaction. This fluid will be continuously subjected to elevated temperatures (500-650°F) under a hydrogen rich atmosphere at high pressure (~1000 psig) in the presence of an active nickel catalyst, and is therefore, subject to both thermally and chemically induced degradation.

For this reason we undertook an experimental program designed to investigate the thermal and chemical stability of commercially available materials which could serve as our heat transfer medium. We have conducted tests on aliphatic oils, paraffin waxes, poly glycols, methylated benzenes, phenyl methyl silicone oils, diphenyl-diphenyl ether eutectic and di- and tri-aryl ether mixtures and salt eutectic mixtures. In addition, the literature has been examined for information on these and other compounds such as chlorinated aromatics, alkylated diphenyl ethers, partially hydrogenated terphenyls and alkyl aromatic oils.

The most common heat transfer fluids are steam and water, and if the temperature is above the freezing point of water or below 350°F, the choice is usually between these two fluids. However, as the temperature increases above 350°F, the vapor pressure of water increases rapidly. Thus with high temperature systems it becomes increasingly important to consider fluids with vapor pressures lower than water.

Some of the more frequently used high temperature organic heat transfer fluids available today are shown in Table 1.

Table 1

Frequently Used Organic Heat Transfer Fluids

Composition	Trade Name	Producer	Usable °F Temp. Range*	
Aliphatic Petroleum Oil	Humbletherm 500	Humble Oil	-5	-600
Alkyl-Aromatic Petroleum Oil	Mobiltherm 600	Mobil Oil	-5	-600
o-Dichlorobenzene	Dowtherm E	Dow Chemical	0**	-500
Diphenyl-Diphenyl Ether Eutectic	Dowtherm A	Dow Chemical	55**	-750
Di- and Tri-Aryl Ethers	Dowtherm G	Dow Chemical	12	-650
Hydrogenated Terphenyls	Therminol 66	Monsanto	25	-650
Polychlorinated Biphenyl	Therminol FR-1	Monsanto	25	-600
Polyphenyl Ether	Therminol 77	Monsanto	50	-700

* The low temperature limit was estimated for each fluid from its minimum pumpability characteristic. This pumping factor has been generally accepted by centrifugal pump manufacturers. It is defined as the temperature where the fluid exhibits a 2000 centipose viscosity.

** This fluid exhibits a true freezing point below the temperature shown. The viscosity at this temperature is less than ten centiposes.

Once the decision has been made to use high temperature heat transfer fluid, the important factors one must evaluate in selecting the fluid are:

1. Toxicity and Environmental Ecology
2. Corrosiveness to Materials of Construction
3. Flammability
4. Thermal Stability and Engineering Properties

III RESULTS OF THERMAL STABILITY TESTS

A. Introduction

Static thermal stability tests of commercial heat transfer fluids are generally conducted under isothermal conditions in sealed pressure bombs. Available data indicate that accelerated tests at high temperatures give sound data on fluid stability while reducing the test time significantly. The degradation products are the same as at normal operating temperatures with the rate of degradation approximately doubling for each 18°F temperature rise (see Figure 1 - one week at 700°F $\cong$ 40 weeks at 600°F).

The progress of degradation may be continuously monitored through changes in bomb pressure during the test period. Residual pressure after cooling indicates the presence of light decomposition products while physical observation of the product liquid for color, odor and solids content gives additional valuable qualitative data. Sample weight losses reported result from either the venting of gaseous decomposition products or from carbon deposits on the wall of the pressure bomb. Nominal handling losses are less than 4%. As a generally recommended guideline to fluid stability, it can be said that if sample loss was $\sim$ 10% in a two to three week period, this corresponds to a weight loss of about ½% to 1% per week at a 50°F lower temperature.

B. Results

The data are presented in two forms: (1) Comparison of physical property changes as in Table 2 and (2) Bomb pressure changes during the test period which are tabulated in Table 3 and graphically presented in Figure 2.

FIGURE 1 *Thermal Stability of Heat Transfer Fluids at Constant Temperature*

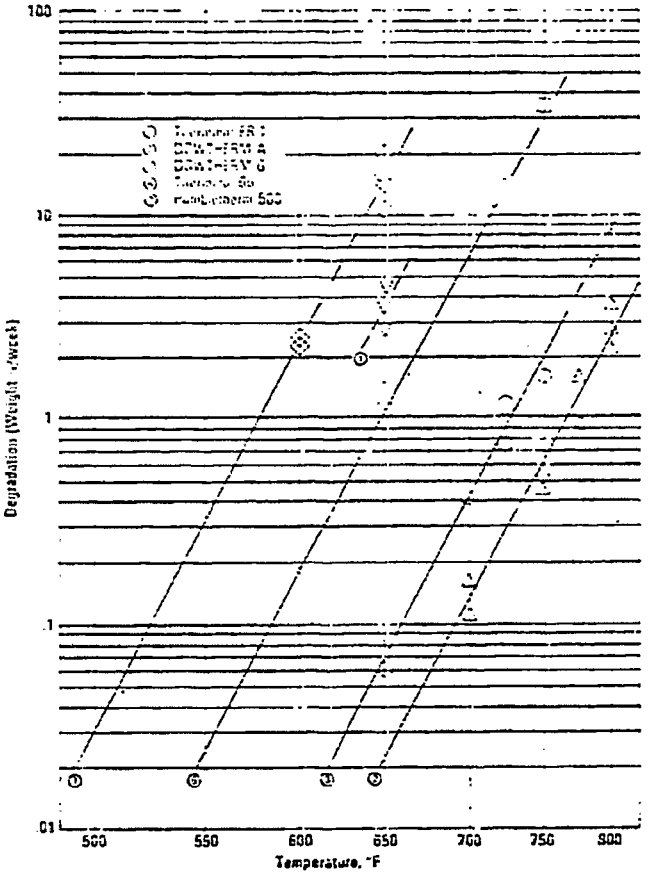

Source: Process Heat Transfer Symposium, 71st National AIChE Meeting, February 22-24, 1972, Dallas, Texas.

Table 2

Static Thermal Stability Comparisons

Material	Length of Test	Temp. °F	Sample Loss %	Physical[a] State	Color	Odor	Residual[b] Pressure psig
1,2,4-Trimethyl Benzene	0	-	-	L	Water-White	Characteristic	-
	4 Days	650	5	L	Pale Yellow	No Change	None
Tetraethylene Glycol	0	-	-	L	Water-White	Neutral	-
	2½ Hours	625	N.A.	L + S	Black	Acrid	10
Diphenyl-Diphenyl Ether Eutectic (1)	0	-	-	L	Pale Yellow	Characteristic	-
	20 Days	625	< 0.5	L	Light Amber	No Change	None
Aliphatic Oil (2)	0	-	-	L	Pale Yellow	Neutral	-
	28 Days	625	~20	L + S	Brown-Black	Acrid	Yes
Petrolatum (3)	0	-	-	S[c]	Opaque White (S) Water White (L)	Neutral	-
	4 Days	650	< 0.5	S[c]	Opaque Amber (S) Amber (L)	Sweet	5
Phenyl Methyl Silicone (4)	0	-	-	L	Water-White	Neutral	-
	9 Days	650	4	L	Very Pale Yellow	No Change	None
$NaNO_3$ - KNO_3	28 Days	650	Nil	L	Pale Yellow	No Change	None

(1) Dowtherm A
(2) Sun 21 Heat Transfer Oil
(3) Penndrake Snow White Petrolatum
(4) Dow Corning 550 Fluid

[a] S-Solids, L-Liquids
[b] Residual Pressure at Room Temperature - 70°F
[c] Naturally Occurring Mixture of Mineral Oil and Micro-Crystalline Wax that is Solid Below 115°F

Table 3

Static Thermal Stability Tests: Bomb Pressure vs. Time

Pseudocumene (650°F)		Penndrake Snow White Petrolatum (650°F)		Dowtherm A (625°F)		Tetraethylene Glycol (625°F)		Dow Corning 550 Phenyl Methyl Silicone (650°F)	
Time	Pressure psig	Time	Pressure psig	Time	Pressure psig	Time	Pressure psig	Time	Pressure psig
				½ hr.	45				
1 hr.	230	24 hrs.	2	17 hrs.	46	45 min.	25	After 9 days at temperature, the pressure was still 0 psig.	
1½ hrs.	240	48 hrs.	18	25 hrs.	53	50 min.	31		
25½ hrs.	235	72 hrs.	30	89 hrs.	50	2 hrs.	72		
45½ hrs.	260	96 hrs.	45	103 hrs.	45	2½ hrs.	100+		
69½ hrs.	235	Residual	5	138 hrs.	47	Residual	10		
93½ hrs.	235			156 hrs.	46				
98½ hrs.	235			247 hrs.	48				
Residual	0			275 hrs.	45				
				299 hrs.	51				
				319 hrs.	50				
				415 hrs.	51				
				Residual	0				

FIGURE 2 : STATIC THERMAL STABILITY TE AT 625°F AND 650°F

BOMB PRESSURE VS. TIME

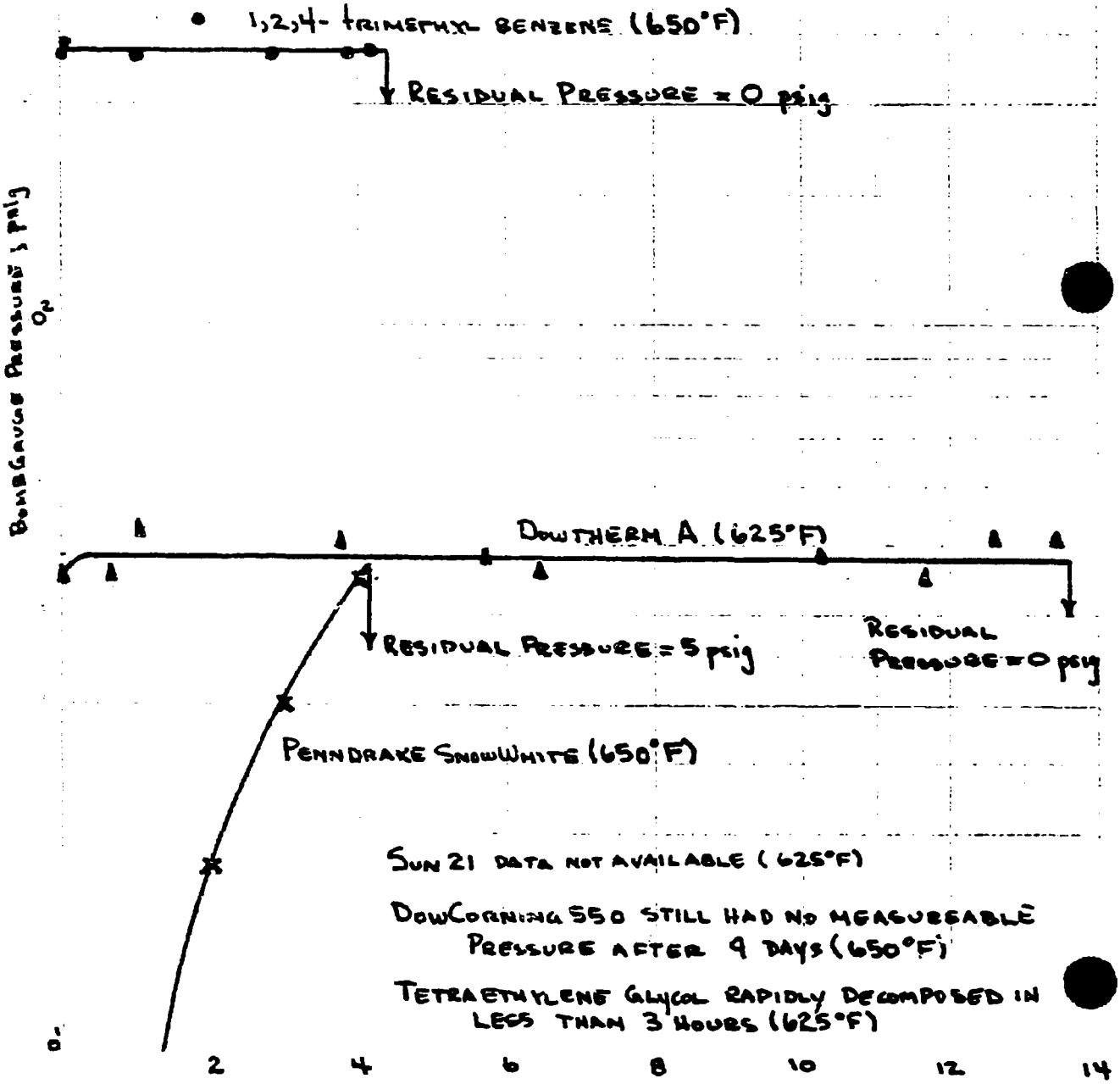

SUN 21 DATA NOT AVAILABLE (625°F)

DOWCORNING 550 STILL HAD NO MEASURABLE PRESSURE AFTER 9 DAYS (650°F)

TETRAETHYLENE GLYCOL RAPIDLY DECOMPOSED IN LESS THAN 3 HOURS (625°F)

Pseudocumene (1,2,4-trimethyl benzene) was stable at a temperature of 650°F as indicated by the absence of light decomposition products (no residual vapor pressure) and the small nominal weight loss, along with minimal changes in physical properties. The only detectable change was a slight coloration from its initial water-white state. Lower methyl benzenes cannot be used because of their higher vapor pressures and lower critical temperatures. Higher polymethyl benzenes (eg. mixed C_{10}s) should behave satisfactorily and might, in fact, be preferable because of their higher viscosities and lower vapor pressures. The viscosity plays an important role in fluidized bed characteristics while lower vapor pressure reduces subsequent solvent vapor-product separations.

Tetraethylene glycol rapidly decomposed at 625°F within only two hours as shown by the rapid rise in bomb pressure (Table 3). After cooling, a residual pressure of 10 psig indicated the presence of light decomposition products while subsequent examination of the liquid showed gross physical property changes. The residual liquid turned black with quantities of fine black, carbon-like particles suspended in it while the odor turned acrid and pungent from its normal, neutral state. There also was a noticeable increase in viscosity indicating that some polymerization had occurred. This is not an uncommon circumstance with poly glycols, which polymerize by a condensation mechanism, eliminating water. Discussions with vendors indicated that poly glycol ethers should perform no better.

The diphenyl-diphenyl ether eutectic mixture (Dowtherm A) was another stable material. Over a three week period at 625°F, the only noticeable change in properties was a slight darkening from its pale yellow color. The manufacturer indicates that this is a natural occurrence. Static thermal stability data available in the literature (Table 4) more than substantiate our findings, indicating that this material is stable at temperatures in excess of 775°F. The literature also points out that aromatic ethers and polyphenyls in general constitute a class of highly thermally stable materials.

Table 4. LITERATURE VALUES
STATIC THERMAL STABILITY COMPARISONS

Compound	Length of Test	Temp. (°F)	Sample Lost-%	Physical State	Color	Resident Pressure
Diphenyl ether—diphenyl[1] eutectic	0	—	—	L	Lt. Yellow	—
	3	775	1.9	L	Yellow	No
Biphenylyl phenyl ether (isomer mixture)	0	—	—	S	White	—
	4	650	2.1	VL	Brown	No
	6	750	5.7	VL	Black	No
	2	775	3.1	VL	Brown	No
	4	775	2.6	VL	Brown	No
o-biphenylyl phenyl ether	0	—	—	S	White	—
	3	750	1.0	VL	Tan	No
	4	775	1.3	VL	Brown	No
m-biphenylyl phenyl ether	0	—	—	L	Yellow	—
	2	775	2.5	L	Brown	No
	4	775	2.3	L	Brown	No
di- and triaryl ethers[2]	0	—	—	L	Yellow	—
	8	650	2-4	L	Brown	No
	4	700	2-4	L	Brown	No
	3	750	2-4	L	Brown	No
	3	775	2-4	L	Brown	No
Dimethyl diphenyl ether[3] (isomer mixture)	0	—	—	L	Colorless	—
	4	650	3.2	L	Brown	No
	3	700	17	L	Black	Yes
	3	750	24	VL	Black	Yes
Tetramethyl diphenyl ether (isomer mixture)	0	—	—	L	Yellow	—
	2	650	1.5	L	Yellow	No
	4	650	1.7	L	Brown	No
	2	700	4.5	L	Black	No
	4	700	8.5	L	Black	No
4,4'-diethyldiphenyl ether	0	—	—	L	Yellow	—
	4	650	3.7	L	Yellow	No
	2	700	12.0	L	Black	Yes

Cont.

1. DOWTHERM® A
2. DOWTHERM® G
3. Dimethyldiphenyl ether (isomer mixture). Diphyl DT. Bayer. Germany

Table 4 —continued
STATIC THERMAL STABILITY COMPARISONS

Compound	Length[a] of Test	Temp. (°F)	Sample Lost-%	Physical[b] State	Color	Residual[c] Pressure
Partially Hydrogenated terphenyl[4]	0	—	—	L	Yellow	—
	8	650	2.5	L	Brown	No
	2	700	10.6	L	Brown	No
	4	700	10.3	L	Brown	Yes
	2	725	9.4	L	Brown	Yes
	4	725	11.9	L	Black	Yes
	1	750	42.7	L&S	Black	Yes
Aliphatic oil[5]	0	—	—	L	Yellow	—
	2	650	8.3	L	Brown	No
	4	650	57.6	L&S	Brown	Yes
Alkylaromatic oil[6]	0	—	—	L	Brown	—
	2	650	8.5	L	Brown	Yes
	4	650	77.2	L&S	Brown	Yes

a—Length of test in weeks
b—Physical state L = Liquid, S = Solid, V = Viscous
c—Residual pressure in reactor at dry ice temperature (−70°C)

4. Therminol 66
5. Humbletherm 500
6. Mobiltherm 600

A paraffinic mineral oil (Sun 21 Heat Transfer Oil) was tested at 625°F for 28 days. The results are unsatisfactory as indicated by the generation of light decomposition products as well as considerable carbonaceous materials. The pale yellow color turned dark brown-black while the ordinarily neutral odor became acrid. In contrast to these results, we have also used this oil in some preliminary high pressure fluidization studies under simulated reactor conditions and found only minor changes in physical properties after cycling the temperature between 70°F and 650°F over a period of two weeks. These changes were a slight darkening of the oil to an amber color and an increased sharpness in odor. Carbonization was not evident. The improved stability under these conditions may be due to the presence of the reducing reaction gases.

As an extension of the work with the paraffinic mineral oil, a petrolatum (Penndrake Snow White Petrolatum), which is a naturally occurring mixture of mineral oil and micro-crystalline wax, was also examined. The evidence is not conclusive but the small residual pressure, barely measureable weight loss and the minor changes in physical properties seems to indicate an increased stability even though the test was run at higher temperature - 650°F as compared to 625°F - a change sufficient to cause more than a doubling of decomposition rates.

A eutectic mixture of $NaNO_3$ and KNO_3 known commercially as Hitec was used as the heating bath for all these tests. Literature indicates it is stable and in use at temperatures up to 700°F. No change in physical properties or appearance was noted for the salt mixture indicating excellent stability.

The last material that was examined is a phenyl methyl silicone oil (Dow Corning 550 Fluid). By all indications, this would be a perfectly satisfactory heat transfer fluid, evidencing only a minor change in the color and a small weight loss after nine days at 650°F. This material

has an extremely low vapor pressure at elevated temperatures (20 mm Hg at 650°F) which reduces solvent vapor carryover and subsequent separation operations. In addition, the silicone oil is almost completely non-toxic under normal industrial handling conditions.

The literature indicates that there is a variety of chlorinated aromatic hydrocarbons which are thermally stable at 600°F. However, decomposition products include hydrogen chloride which would present unnecessary corrosion problems.

IV CONCLUSIONS AND RECOMMENDATIONS

We have investigated the thermal stability of a variety of commercially available heat transfer fluids and have shown that there are at least four classes of materials which possess sufficient thermal stability at temperatures in excess of 650°F to be successful candidates for the next phase of the research program. The candidates are:

1. Aromatic Ethers
2. Polymethyl Aromatics
3. Inorganic Salts
4. Phenyl Methyl Silicone Oils

We have also shown that purely paraffinic materials are stable up to temperatures of 600°F. The only material that conclusively failed the thermal stability test was tetraethylene glycol. In this case, degradation products included fine carbonaceous material as well as polymerization products, probably higher molecular weight poly glycols.

The aromatic ethers include the commercially available Dowtherm A (diphenyl-diphenyl ether eutectic), Dowtherm G (di- and tri-aryl ethers), Diphyl DT (dimethyl diphenyl ether isomers) and other substituted aromatic ethers. These materials are intermediate in cost, ranging from about $0.15 to 0.30/lb. Their physical properties are such that heat can be removed as both sensible and latent heat. Because they are non-corrosive, carbon steel is the normal material of construction. Vapor pressures at process conditions are moderate.

Alkyl aromatics are low in cost, about $0.04 to 0.06/lb for a C_9 or C_{10} crude cut. The low cost affords us the freedom of greater solvent losses which will likely occur due to their greater volatility.

Through normal blending techniques, liquid properties can be optimized for a particular operating condition and heat removal can be in both sensible and latent forms. These materials are non-corrosive and carbon steel is the normal material of construction.

Inorganic salts, such as the sodium nitrate/potassium nitrate mixture, are also moderately low in cost, about $0.12/lb. They are the most stable of the fluids tested but require more complicated piping, startup and shutdown procedures because of their high melting point. Water dilution techniques are available to reduce or eliminate these problems and they are therefore still attractive classes of heat transfer fluids. Experience has shown that these materials are non-corrosive to carbon steel. An additional plus in their favor is their negligible vapor pressure which eliminates the contamination of product gases with solvent vapor and subsequent separation operations.

Phenyl methyl silicones are a very stable class of fluids. Their stability increases with increasing phenyl content which can vary from zero to over fifty percent. They are expensive materials, about $4.50/lb. However, their negligible vapor pressure (20 mm Hg at 650^{o}F) reduces solvent vapor losses to a minimum with a concurrent low operating cost due to solvent make-up. In a 250 MM cubic feet/day plant requiring a solvent inventory of about 15,000 gallons, a 0.5%/week solvent loss rate, which is probably the upper bound, would be equivalent to 0.15 cents per thousand cubic feet of methane produced. In addition, these materials are almost completely non-toxic under industrial operating conditions. They are non-corrosive requiring only carbon steel as a construction material and have simple startup procedures since they remain liquid at temperatures down to -58^{o}F. Heat removal is in the form of sensible heat only.

If the actual process design temperatures are below 650^{o}F, paraffinic heat transfer fluids become a very attractive alternative. They are

inexpensive, from $0.04 to 0.11/lb, costing about the same as the polymethyl benzenes and inorganic salts. They have the distinct advantage, when compared to the polymethyl benzenes, of having a negligible vapor pressure at process conditions which greatly simplifies solvent recovery and product purification. In addition, their advantage over the inorganic salt lies in their simpler startup and shutdown procedures.

Combining the factors of cost, ease of use and process implications in a non-qualitative way leads us to feel the order of preference for these materials is:

Diphenyls
Polymethyl Aromatics
$NaNO_3$ - KNO_3
Silicone Oils

* ASTM

APPENDIX I

Experimental Apparatus and Procedure

A. Equipment

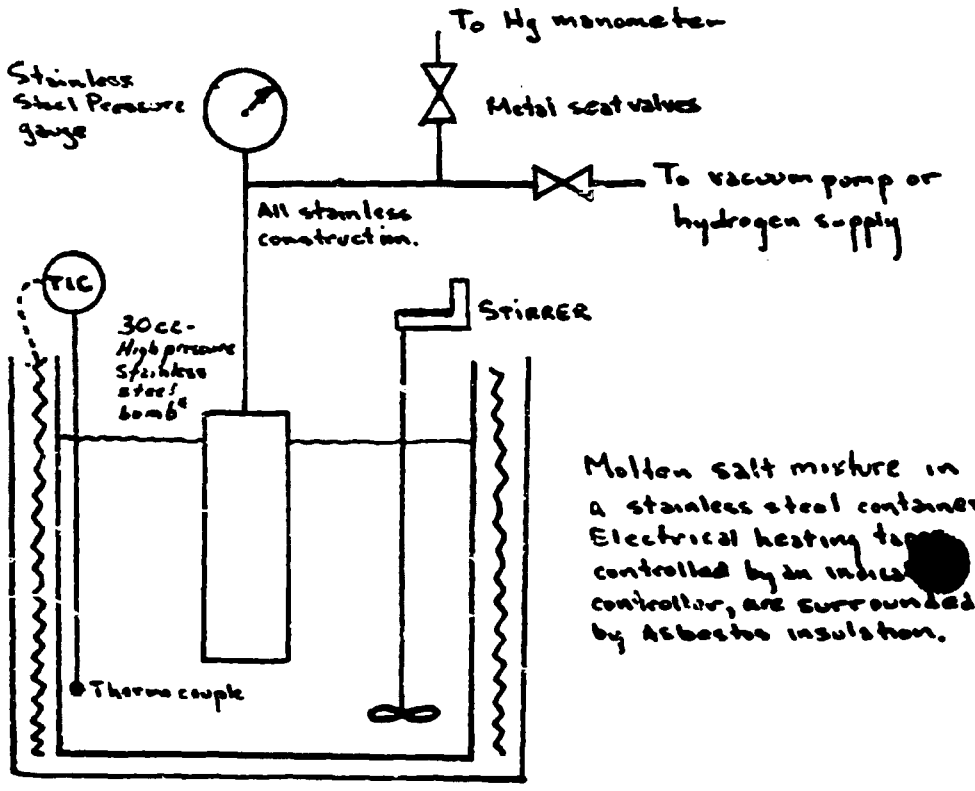

* The salt bath can contain up to four test bombs at a time.

FIGURE AI-1 EXPERIMENTAL APPARATUS

B. Procedure

1. Pressure bomb is cleaned with Chromerge solution for six hours.
2. Pressure bomb, valves, tubing, fittings and gauge are all soap and water washed, water rinsed, acetone rinsed and oven dried at 110°C.
3. All the equipment is assembled except for the bomb, using Teflon pipe tape on all pipe threads.
4. The sample and catalyst, if necessary, are weighed directly into the bomb.
5. The assembly is completed by screwing on the bomb, then it is evacuated with the vacuum pump while monitoring on the Hg manometer. The system is isolated from the vacuum pump and leaks are detected by loss of vacuum during a three hour period.
6. If hydrogen is to be added, it is done so at this time using the same line as for the vacuum pump. Valve to manometer is closed and bomb is pressurized to 200 psig hydrogen. System is closed and examined for leaks by monitoring gauge pressure over a three hour period.
7. The bomb is placed slowly in salt bath to prevent rapid expansion of joints which might cause leaks.

C. Observations

1. At regular intervals, the pressure and temperature are recorded.
2. At the end of the test period, the bomb is removed from the salt bath and allowed to cool to room temperature. Residual pressure, if any, indicates gaseous degradation products.
3. Analysis of gas is attempted in order to identify some of the components from hydrogen up to butanes.
4. After the bomb is vented, it is weighed to determine weight loss.
5. The residual liquid sample is recovered and examined chromatographically to determine liquid degradation products (lighter or heavier than original material).
6. The liquid is also examined for color, odor and feel and the bomb is examined for carbonaceous residue.

APPENDIX II

Bulk Prices of Heat Transfer Fluids

Table AII-1

	Bulk Price
Sun 21	$ .045/lb
Dowtherm A	$ .36 /lb
Dowtherm G	$ .31 /lb
Penndrake Code 4417	$ .115/lb
Penndrake Drakeol 19	$ .115/lb
Penndrake Snow White Petrolatum	$ .103/lb
Dow Corning 510	$ 4.22 /lb
Dow Corning 550	$ 4.65 /lb
Fluorinated Hydrocarbons	$ 5.00-8.00 /lb
Pseudocumene (C_9 Methyl Benzene)	$ .06 /lb
C_{10} Methyl Benzene Isomers	$ .04 /lb

APPENDIX III

Physical and Thermal Properties of Heat Transfer Fluids

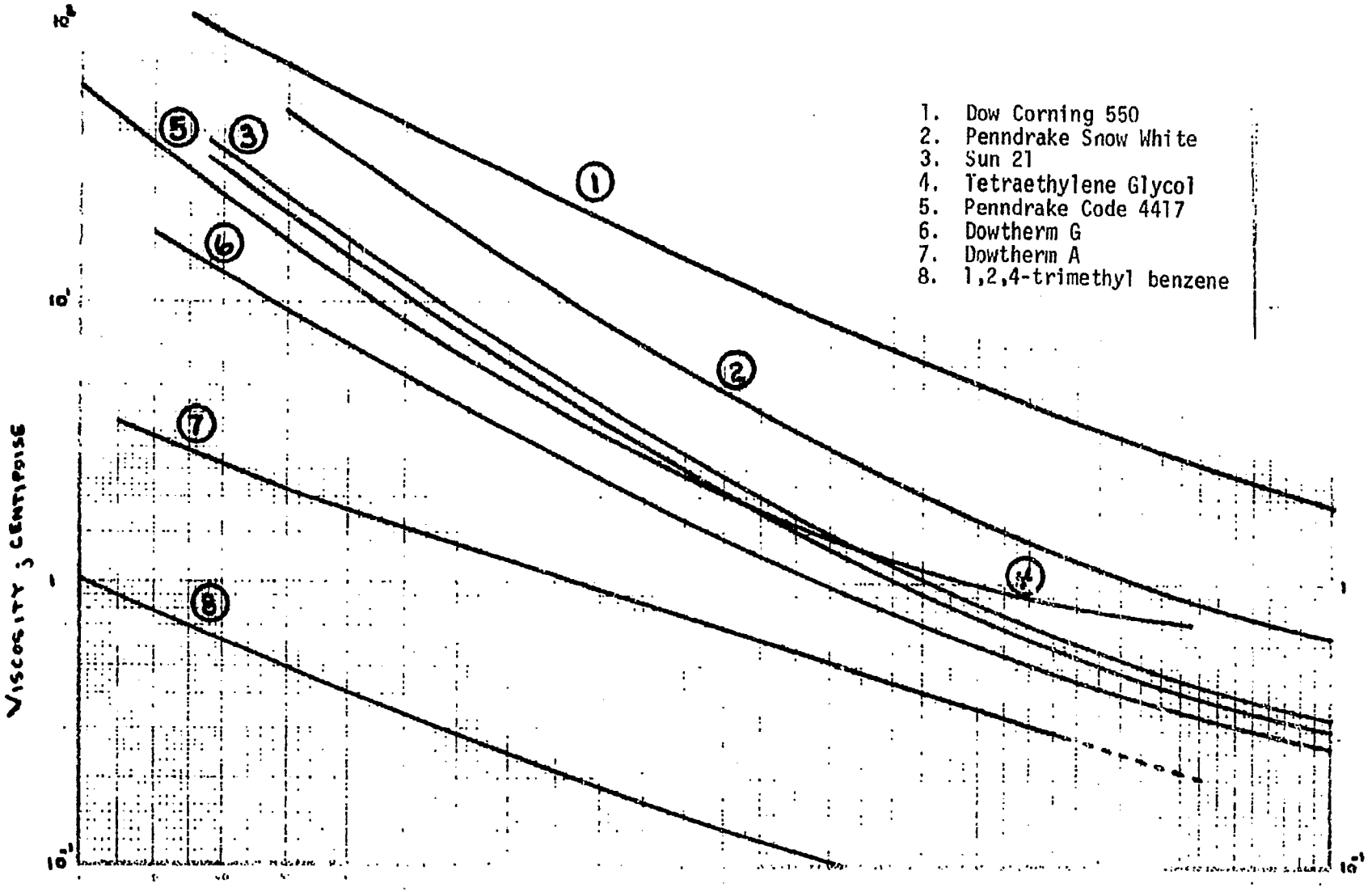

Figure AIII-1

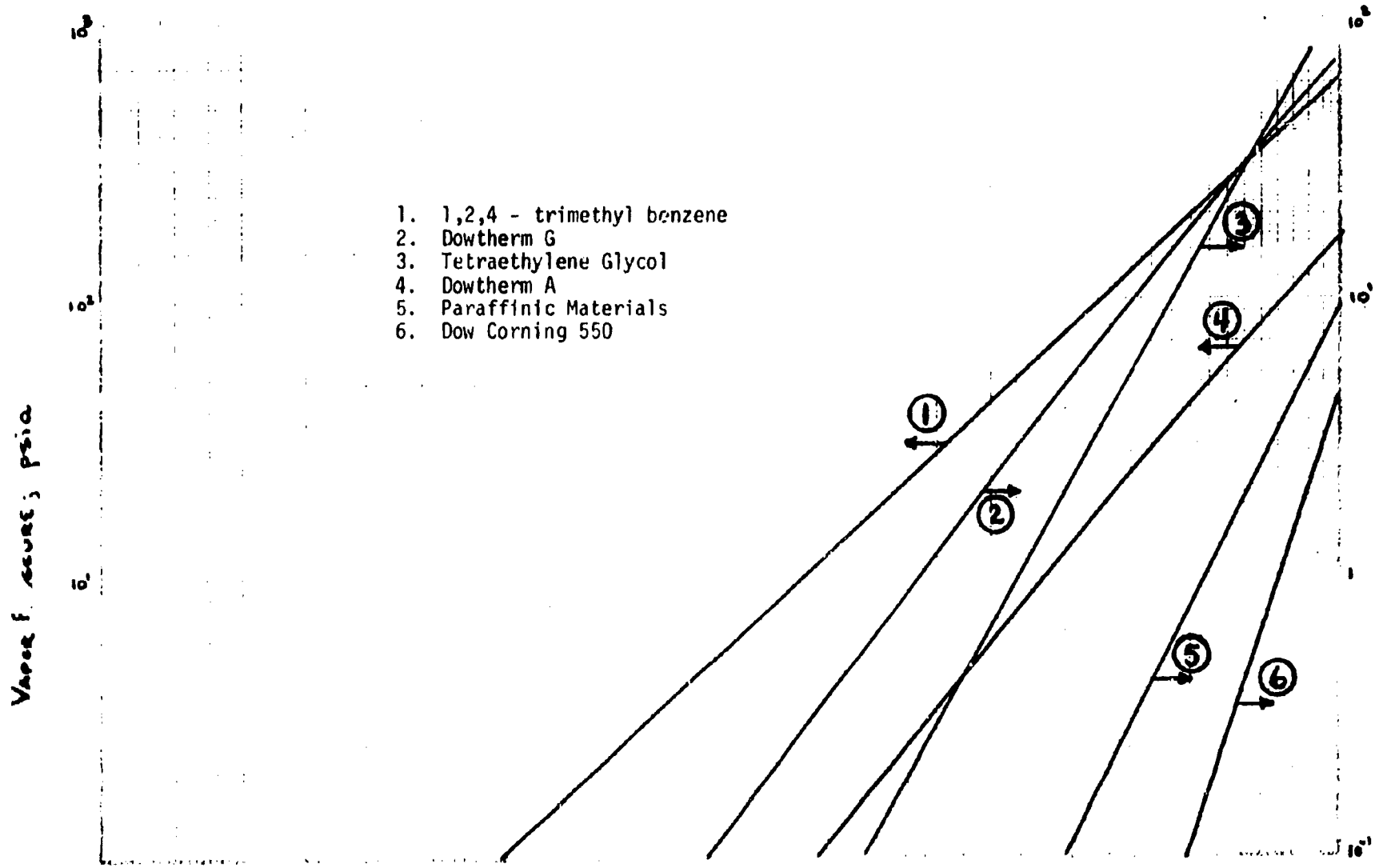

FIGURE AIII-2

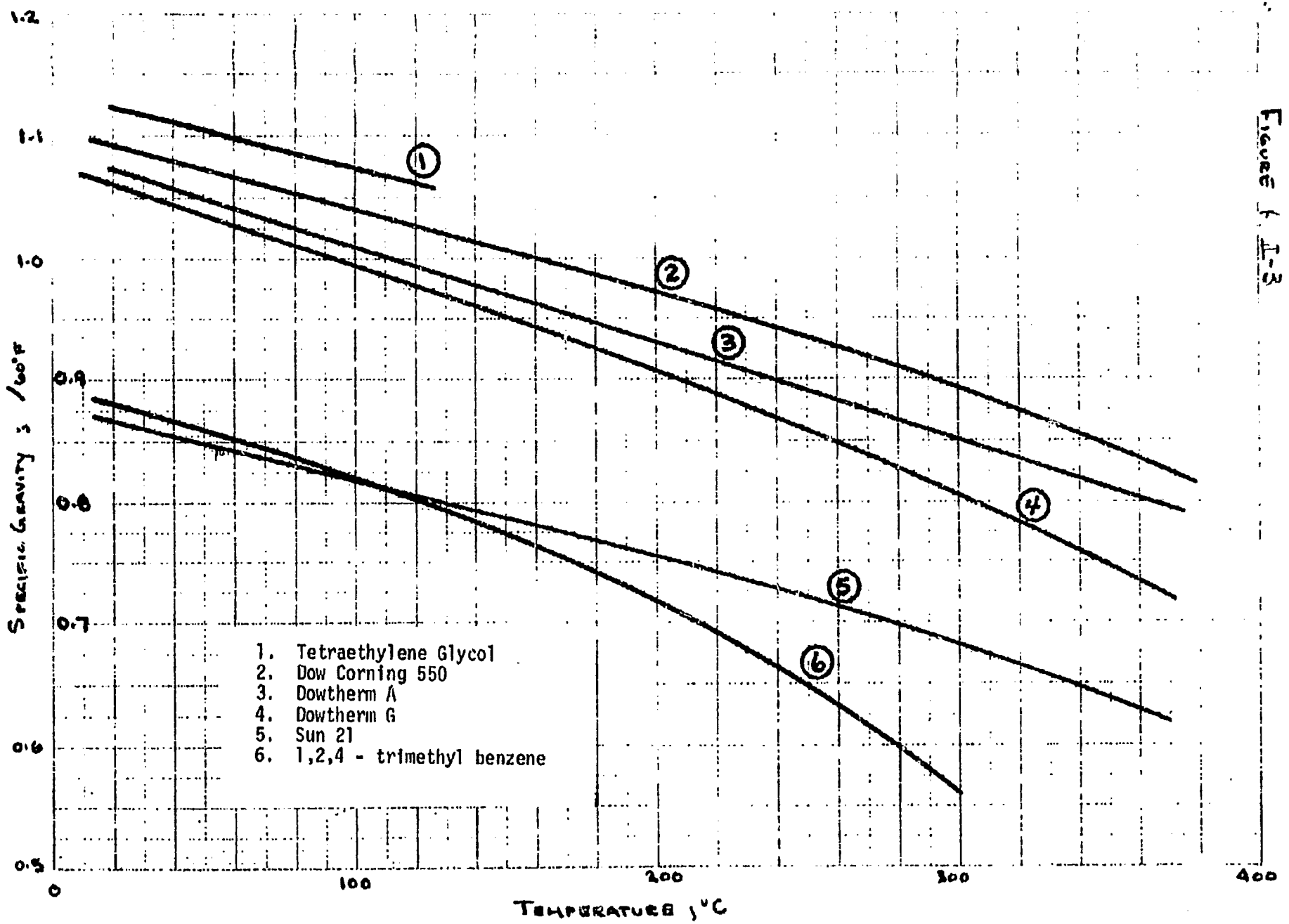
1.2
1.1
1.0
0.9
0.8
0.7
0.6
0.5
SPECIFIC GRAVITY @ 60°F
0
100
200
300
400
TEMPERATURE °C
1. Tetraethylene Glycol
2. Dow Corning 550
3. Dowtherm A
4. Dowtherm G
5. Sun 21
6. 1,2,4 - trimethyl benzene

FIGURE I-3

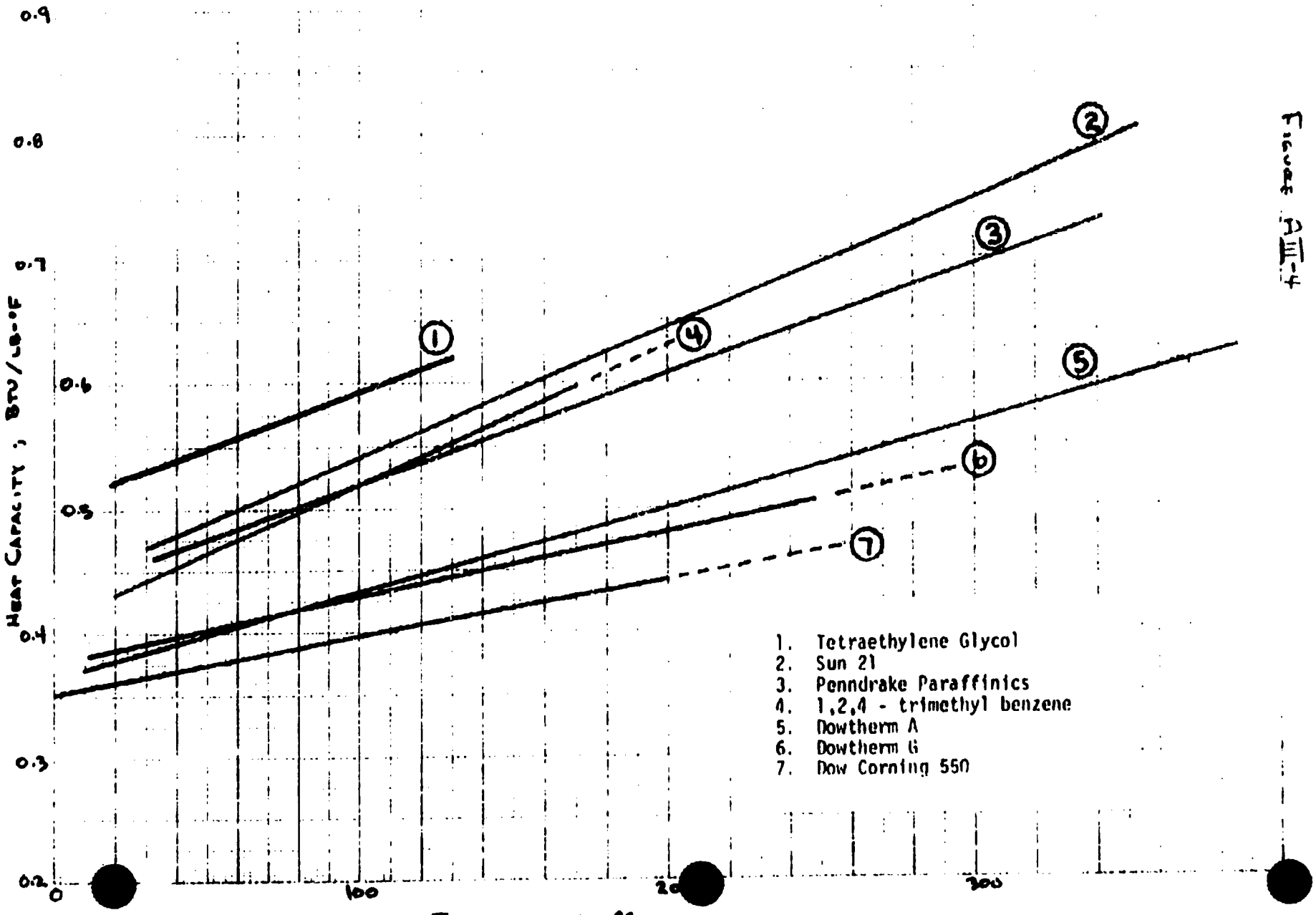
0.9
0.8
0.7
0.6
0.5
0.4
0.3
0.2
0
100
200
300
HEAT CAPACITY ; BTU/LB-°F
1
2
3
4
5
6
7
1. Tetraethylene Glycol
2. Sun 21
3. Penndrake Paraffinics
4. 1,2,4 - trimethyl benzene
5. Dowtherm A
6. Dowtherm G
7. Dow Corning 550

Figure III-4

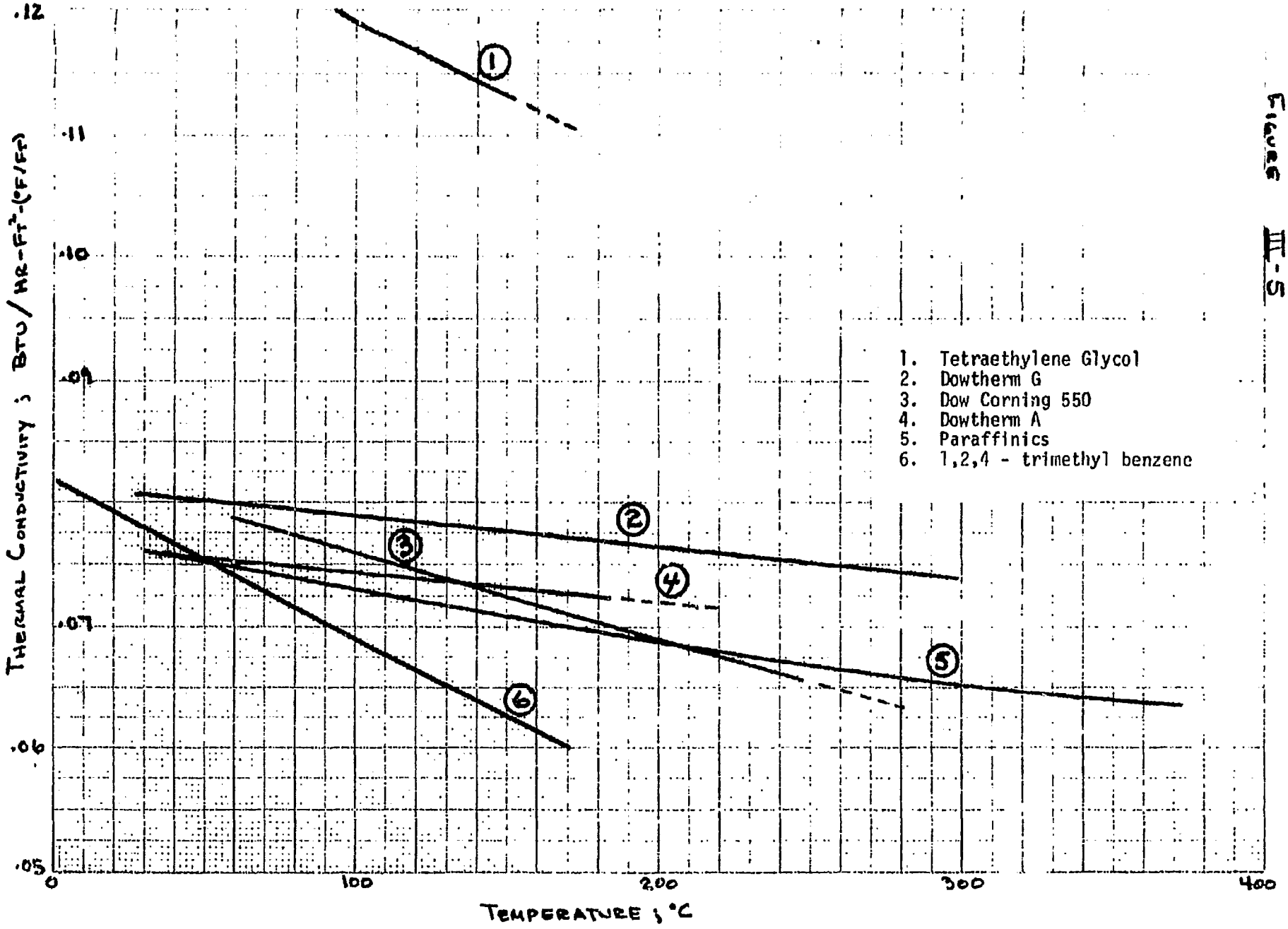
.12
.11
.10
.09
.07
.06
.05
0
100
200
300
400
THERMAL CONDUCTIVITY ; BTU/HR-FT²-(°F/FT)
TEMPERATURE ; °C
1. Tetraethylene Glycol
2. Dowtherm G
3. Dow Corning 550
4. Dowtherm A
5. Paraffinics
6. 1,2,4 - trimethyl benzene

Figure III-5

Table AIII-1

PHYSICAL AND THERMAL PROPERTIES

TEMP DEG F	1 DTG	2 DTA	3 TFR1	4 HBL500	5 MBL600	6 T66	7 DTE	HITEC SALT	WATER
SPECIFIC HEAT BTU (LB)(FT)									
100	0.3950	0.3880	0.2930	0.4850	0.3800	0.3750	0.281	solid	1.00
200	0.4200	0.4260	0.3047	0.5333	0.4380	0.4300	0.303	solid	1.00
300	0.4540	0.4630	0.3255	0.5791	0.4850	0.4700	0.328	0.373	1.03
400	0.4760	0.5000	0.3484	0.6249	0.5320	0.5300	0.357	0.373	1.08
500	0.5100	0.5370	0.3672	0.6707	0.5780	0.5700	0.383	0.373	—
600	0.5410	0.5760	0.3830	0.7165	0.6250	0.6300	0.410	0.373	—
700	0.5670	0.6110	0.4029	0.7623	0.6710	0.6800	0.440 est	0.373	—
VISCOSITY LB/(FT)(HR)									
100	36.2000	6.2500	72.5000	56.4000	136.0000	72.0000	2.500	solid	1.620
200	7.0200	2.5700	9.2340	12.4000	15.2500	10.1500	1.600	solid	0.725
300	2.9000	1.4000	3.4150	4.5400	4.8400	3.7600	0.970	43.6	0.485
400	1.6500	0.9000	1.8900	2.6200	2.9300	1.9800	0.655	18.1	0.330
500	1.0600	0.6500	1.2300	1.4100	1.4600	1.0800	0.510	10.2	—
600	0.7700	0.4800	0.9000	1.0100	0.9510	0.7490	0.433	7.25	—
700	0.6000	0.3600	0.7070	0.7000	0.5350	0.5490	0.350 est	5.32	—
THERMAL CONDUCTIVITY BTU/(HR)(FT²)(°F/FT)									
100	0.0755	0.0805	0.0608	0.0775	0.0695	0.0703	0.0685	solid	0.397
200	0.0742	0.0765	0.0597	0.0750	0.0675	0.0685	0.0645	solid	0.392
300	0.0731	0.0725	0.0587	0.0725	0.0653	0.0670	0.0607	.33	0.387
400	0.0720	0.0685	0.0576	0.0705	0.0631	0.0657	0.0567	.33	0.382
500	0.0706	0.0645	0.0563	0.0675	0.0611	0.0640	0.0528	.33	—
600	0.0693	0.0607	0.0549	0.0655	0.0586	0.0620	0.0490	.33	—
700	0.0681	0.0568	0.0533	0.0638	0.0566	0.0605	0.0450 est	.33	—
DENSITY LB/FT³									
100	68.0000	65.2700	85.5000	53.0000	58.4000	61.7000	80.30	solid	62.0
200	65.2400	62.4600	82.2000	50.7500	56.2700	59.3000	76.40	solid	60.4
300	62.4900	59.5000	78.7600	48.6100	54.2600	56.7000	72.20	123.0	57.3
400	59.6200	56.6700	75.2400	46.4200	52.1600	53.7000	67.70	121.0	53.7
500	57.1200	53.0000	71.8000	44.2400	50.1700	50.5000	62.60	118.0	—
600	54.2500	49.2900	68.3600	41.3100	48.1100	48.1000	56.60	115.0	—
700	51.4000	45.0300	64.9200	39.1200	45.9800	45.6000	51.00 est	113.0	—

1 Dowtherm G

2 Dowtherm A

3 Therminol FR-1

4 Humbletherm 500

5 Mobiltherm 600

6 Therminol 66

7 Dowtherm E

APPENDIX IV

Engineering Properties of Heat Transfer Fluids

*Relativ eat Transfer Film Coefficient vs Temperature**

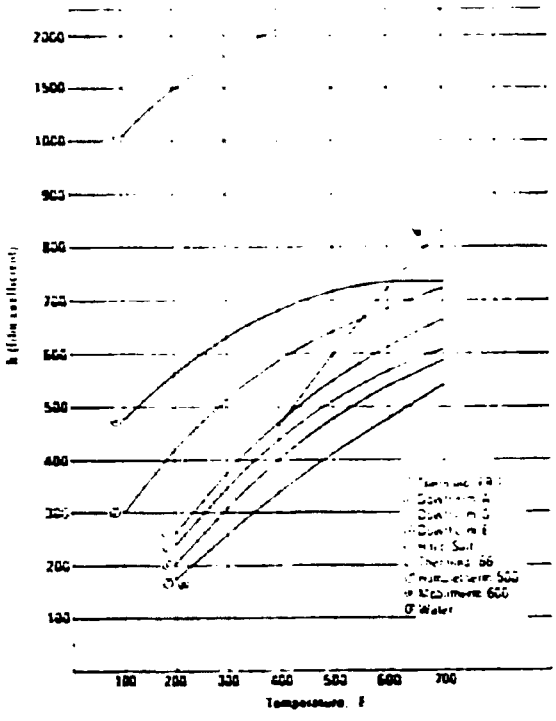

*Relative Horsepower vs Temperature** (Heat Transfer Fluid Film Controlling)

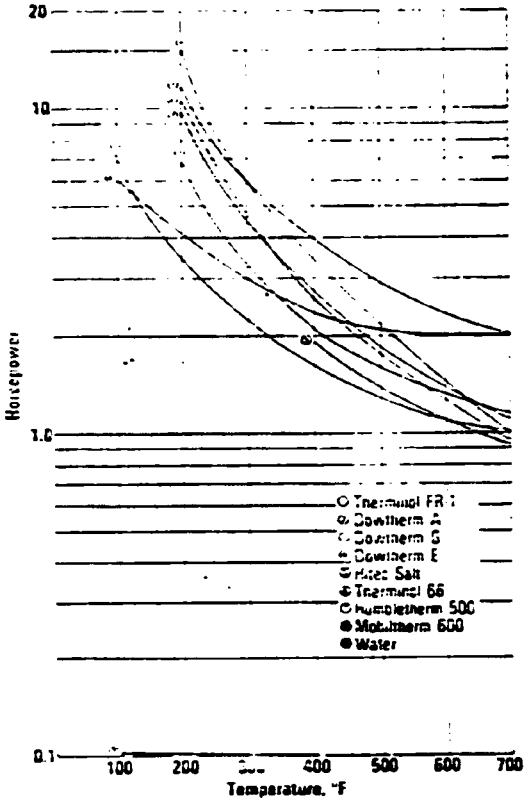

FIGURE AIV-3

*Relative Horsepower vs Temperature** (Process Fluid Film Controlling)

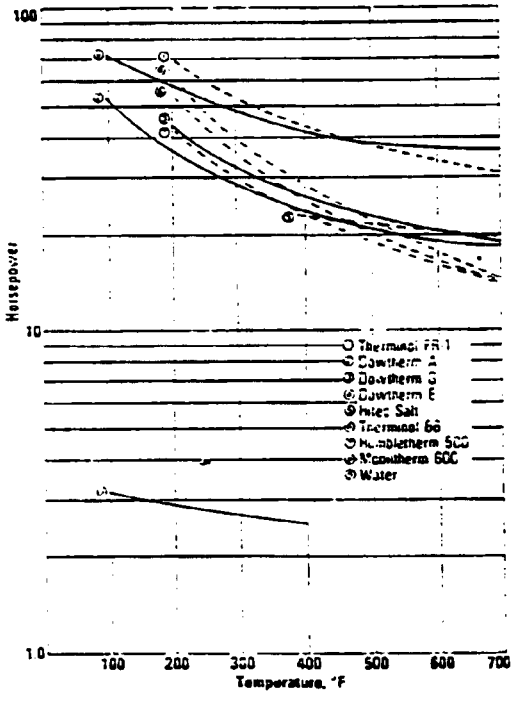

* Absolute ratios between fluids will not be affected significantly by changing the physical dynamics of the system (i.e., tube diameter, fluid velocity, temperature differential between fluids, etc.).

CSI-MPR--2

Chem Systems Inc.

LIQUID PHASE METHANATION

Progress Report No. 2
Fluidization Studies and
Literature Review

Prepared By Chem Systems Inc.

For The American Gas Association

July, 1972

TABLE OF CONTENTS

I SUMMARY

This report includes studies executed prior to the formal contract date and concerns itself with additional significant features of the proposed liquid phase methanation process other than liquid phase thermal stability.

Liquid-Gas-Solid Fluidization

During the past months we have examined the important aspects of liquid-gas-solid fluidized beds from both a theoretical and an experimental point of view. The actual mechanics of the fluidized bed as well as the characteristic heat and mass transfer mechanisms have been emphasized illustrating the relative advantages over alternative systems.

In general, at low superficial gas velocities ($\lesssim 1$ cm/sec), the liquid phase is the dominant force in fluidization and the bed behavior can be described solely in terms of liquid and solid phase properties. The relative importance of the liquid and gas phase can best be described by considering an equation of the form:

$$\epsilon = k\, u_l^a\, u_g^b$$

where ϵ is the bed porosity and u_l and u_g are the superficial liquid and gas velocities.

For our work with irregularly shaped catalyst particles, the values of the exponents a and b were respectively 0.16 and 0.0 at superficial gas velocities less than 0.6 cm/sec. The gas rate exponent increased to 0.085 for superficial gas velocities between 2.0 and 12.0 cm/sec. Other investigators found a stronger dependence of liquid flow with values of the exponent a ranging between 0.4 and 0.6 for regular

between the single sphere and packed bed value.

Wall to bed heat transfer has been examined by several investigators and they observe that the heat transfer coefficient, h_w varies with porosity, ε, in such a way as to give a maximum value in heat transfer coefficient at a particular intermediate porosity. This is probably a result of the opposing effects (which arise with increasing bed porosity) of increased particle velocity, which reduces wall film thickness and decreases particle concentration in the bulk.

Mass transfer studies have followed the same lines of reasoning used in studying the analogous heat transfer problem. Extension of the single sphere mass transfer case results in values for fluidized bed mass transfer coefficients intermediate between the single sphere and packed bed values. On the other hand, wall mass transfer coefficients are 5-10 times the no-solids case at comparable flow rates. We note that there are difficulties in dissolution mass transfer studies arising from induced roughness at the surfaces, which can cause erroneous results. These problems have been overcome by the use of ionic mass transfer experiments, where there is no loss of diffusing species due to reaction at the electrodes.

Comparisons between overall mass transfer coefficients and overall heat transfer coefficients through the use of the Colburn analogy are inadequate when the Schmidt number is very much greater than the Prandtl number which results in a relatively large bed heat transfer resistance when compared to the bed mass transfer resistance, which is negligible.

Flow Behavior

Flow studies in three phase fluidized beds have been limited to the study of bed expansion, bubble properties and mixing patterns. The main complexity in describing the bed behavior arises from both bubble

spherical particles. Their gas flow exponent b values were very similar to ours, ranging from 0.06 to 0.08.

Through the use of a proposed correlation technique involving a reduced liquid velocity, u_l/u_t, where u_t is the particle terminal velocity, we were able to predict bed porosity in a fixed geometric system over a wide range of process conditions for a variety of liquid/gas combinations from simple experiments at ambient conditions. This greatly simplifies future data reduction by giving us a reliable estimate of actual bed expansion and porosity values for the closed reaction system. Theoretical correlations for minimum fluidization velocity and fluidized bed pressure drop were inadequate in this study because of their inability to account for, in a simple manner, the wide particle size and shape distributions used. However, they do show the correct trends in all cases.

Heat and Mass Transfer

In many applications of fluidized beds, the addition or removal of heat from the bulk of the bed is a prime consideration, especially so in the highly exothermic reaction under consideration. There are three pertinent modes of heat transfer: (1) convective transfer between points in the bed caused by mixing, (2) surface heat transfer between particle and fluid, and (3) transfer between the bulk of the bed and the wall. The first two modes produce an effective heat conduction or diffusion in the bed while the third one provides a means of adding or removing heat from the bulk.

Studies on heat transfer from the particle to the bulk are based on an extension of the single sphere heat transfer case to first, packed, and then, fluidized beds. There is a wide variation in the available fluidized bed data, however, all the researchers have found that there is a sharp drop in Nusselt number at particle Reynolds numbers less than 100. For Reynolds numbers greater than 100, the Nusselt number lies

coalescence, which is prominent in beds which are mildly fluidized, and the tendency of bubbles to migrate towards the center of the tube as they rise. As a result, bubble velocity is a complex function of both liquid and gas flow rates; further, there is also a strong dependence on bed porosity. An important consequence of changes in bubble velocity is its effect on gas holdup. At low gas flow rates ($u_g < 1.0$ cm/sec), gas holdup is small, on the order of 5%. Even at a gas flow rate of 8.5 cm/sec, gas holdup will only increase to about 15%.

The interactions between the three phases result in very definite axial and radial mixing patterns. For the most part, radial mixing is complete and there is a definite circulation pattern established, with particles slowly rising in the center and moving downward at the walls. Axial mixing (backmixing) is increased by increased gas flow and decreased liquid flow. Most interesting was the observation that the presence of a solid phase reduces axial mixing by 50-70% over the no-solids case.

Commercial Methanation and Analogous Liquid-Gas-Solid Fluidized Bed Processes

With the advent of coal gasification, methanation of high concentration CO streams becomes a necessity. The crucial problem inherent in the methanation step is the large amount of heat evolved by the reaction which required complicated and expensive schemes to remove the heat. Consequently, most of the research in this area has been directed towards improved heat removal methods.

The basic reaction, as given below,

$$CO + 3H_2 \rightleftharpoons CH_4 + H_2O$$

is catalyzed by a variety of catalysts; nickel based catalysts being the most prominent commercially. Side reactions leading to the formation of CO_2 and C are important only at temperatures greater than 350°C.

Among the various alternatives proposed as solutions to the heat removal problem are (1) introduction of cold feed gas at different points in the reactor train, (2) recycle of large quantities of product gas, (3) gas-solid fluidized bed reactors and (4) tube wall reactors where the catalyst is bonded to the tube wall.

Economic evaluations of all the various processing alternatives show that the methanation step is the expensive one. The difference in economics of the product recycle case and interreactor quench case are relatively small, with operating costs of about 4¢/MSCF in a 250 MM SCFD plant. Capital cost for this plant would be on the order of thirteen million dollars. Gas fluidized bed economics clearly result in lower reactor costs if the process scheme is commercialized.

The advantages of the liquid phase methanation system lies in both economics and reliability. The economic advantages are related to both reduced capital and operating costs arising from the simplified reactor design. Additional advantages are that heat removal is more efficient and therefore results in a decrease in necessary heat transfer area. Also, use of a concentrated feed, up to 20% CO, results in substantially increased productivity volume of equipment which reflects itself in a reduction in the power costs which form a large part of the operating costs. Reliability is enhanced by the ability to prevent temperature runaway in the large heat sink and the ability to treat the catalyst without shutdown.

The motivation for the proposed liquid phase methanation process is based largely on expertise developed for the analogous three phase reaction systems; Fischer-Tropsch Synthesis and the H-Oil Process. The Fischer-Tropsch process went through several stages of development differing chiefly in the modes of heat removal. Final designs operated by I. G. Farbenindustrie in Germany prior to World War II utilized a submerged iron catalyst bed fed by a $CO-H_2$ gas mixture. Convector volumes of 7 to 50 cubic feet were successfully operated but further commercial development was halted because of the war.

BLANK PAGE

Subsequent work by the Bureau of Mines found that performance could be greatly improved if a mildly fluidized air of 10-40 mesh catalyst particles was used.

In the H-Oil process, the motion of the catalyst with the high oil velocity results in an intimate contact between oil, hydrogen and catalyst, making the system very efficient with respect to the amount of catalyst charged per unit of oil throughput. The cushioning effect of the oil phase reduces catalyst attrition, and further, the catalyst is retained within the volume of the reactor so that it is unnecessary to provide for catalyst product separation. An additional advantage is the possibility of semi-continuous addition and removal of catalyst.

The relevance of the Fischer-Tropsch and the H-Oil systems is largely related to their similarity in scale which indicates that numerous common problems will exist. The knowhow derived from the above mentioned processes will be extremely valuable in the development stage of the liquid phase methanation system.

Analytical System

Lastly, the report reviews the important features necessary for accurate analysis of the gas reaction system, indicating the need to separate and quantify CO, CO_2, CH_4 and other light hydrocarbons as well as H_2 and H_2O.

II INTRODUCTION

Chem Systems is, under sponsorship of the American Gas Association, developing a new methanation process capable of single pass high conversions of high concentration CO streams. The proposed liquid phase methanation process involves a liquid flowing cocurrent to the gas which serves both to fluidize the catalyst bed and to remove the heat evolved by the methanation reaction. The liquid phase thermal stability aspect has been examined and reported on in our Progress Report No. 1. [1] In this report, we are covering studies performed prior to our formal contract's executions in the areas of three phase fluidization, a methanation review and an experimental analytical design.

Here we are concerned with the effects that various design parameters (eg. liquid density and viscosity, catalyst particle geometry, liquid and gas flow rates, and gas density) might have on the fluidized bed behavior. A search of the literature has shown that some experimental work has been done on liquid-gas-solid fluidization. This material has been analyzed and is presented as a basis for comparison with our experimental results along with the standard theoretical analyses. In addition, this report examines the other important aspects of fluidized bed behavior with emphasis on heat and mass transfer, flow and mixing patterns and present industrial applications (eg. Fischer-Tropsch and H-Oil processes).

A general review of the methanation of synthesis gas is also presented and includes present catalyst systems as well as commercial alternatives to the proposed liquid phase methanation process.

Lastly, the report concerns itself with the development of an analytical system capable of evaluating the reaction system gases in a quantitative manner.

III PRESENTATION OF RESULTS ON THREE PHASE FLUIDIZATION

In this section, experimental data generated both in-house and by other investigators are presented.

A. Introduction

1. Theoretical Background

Fluidization data are generally presented in terms of bed expansion ratios, or voidage fraction, as a function of flow rates. In addition, pressure drop data are helpful in cases where visual observation of the bed is impossible, since it is indicative of fluidization behavior.

Bed expansion ratios are defined as the height of the bed under flow conditions relative to the height of the bed at incipient fluidization (which corresponds to the loosest packing case). Voidage in fluidized beds can be obtained from bed expansion ratios using the relationship:

$$\frac{H}{H_{mf}} = \frac{1-\epsilon_{mf}}{1-\epsilon} \qquad \begin{aligned} \epsilon_{mf} &= \text{Voidage at Minimum Fluidization Velocity} \\ \epsilon &= \text{Voidage at a Given Condition} \end{aligned} \qquad (1)$$

Pressure drop through the bed can be used as an indicator of bed activity, as shown by the following argument. As long as the bed is dormant, pressure drops can be predicted by the Ergun equation:

$$\frac{\Delta P}{H} g_c = 150 \frac{(1-\epsilon)^2}{\epsilon^3} \frac{\mu u_o}{(\phi_s d_p)^2} + 1.75 \frac{1-\epsilon}{\epsilon^3} \frac{\rho_L u_o^2}{\phi_s d_p} \qquad (2)$$

where the first term represents viscous losses and the second term, kinetic losses. Fluidization will occur when the drag force of the upward moving fluid (equivalent to the product of the pressure drop and the cross-sectional area of the tube) balances the weight of the particles, or:

$$\Delta P A = W = (A H_{mf}) (1-\epsilon_{mf}) (\rho_s - \rho_L) (g/g_c) \qquad (3)$$

Rearranging equation 3, we have:

$$\frac{\Delta P}{H_{mf}} = (1-\epsilon_{mf}) (\rho_s - \rho_L) (g/g_c) \qquad (4)$$

BLANK PAGE

At incipient fluidization, the pressure drops predicted by equations 2 and 4 are the same. The superficial velocity at minimum fluidization can therefore be obtained from the following expression:

$$\frac{1.75}{\phi_s \epsilon_{mf}^3}\left(\frac{d_p\, u_{mf} \rho_L}{\mu}\right)^2 + \frac{150\,(1-\epsilon_{mf})}{\phi_s^2 \epsilon_{mf}^3}\left(\frac{d_p\, u_{mf} \rho_L}{\mu}\right) = \frac{d_p^3 \rho_L (\rho_s - \rho_L)}{\mu^2} \qquad (5)$$

where:

d_p : Equivalent Particle Diameter, cm

u_{mf} : Minimum Fluidization Velocity, cm/sec

ϵ_{mf} : Voidage at Incipient Fluidization

μ : Liquid Viscosity, poise

ϕ_s : Sphericity

ρ_L : Liquid Density, gr/cm^3

ρ_s : Solid Density, gr/cm^3

With velocities beyond minimum fluidization, the pressure drop remains practically unchanged. This behavior is shown below.

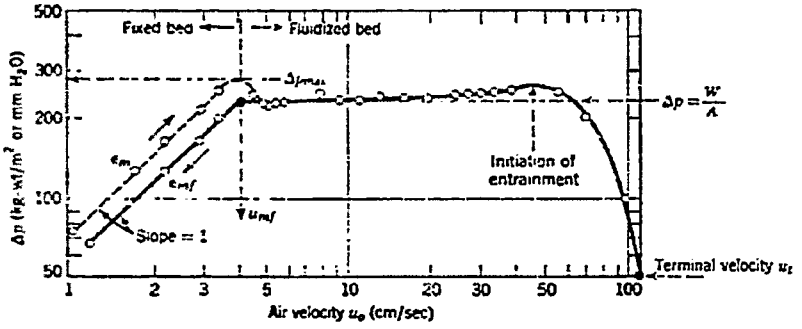

Figure III-1 Pressure Drop Behavior in a Normal Fluidized Bed

Abnormal behavior in fluidized beds can generally be detected by a pressure drop-velocity curve. For example, slugging and channelling will give the following type of relationships.

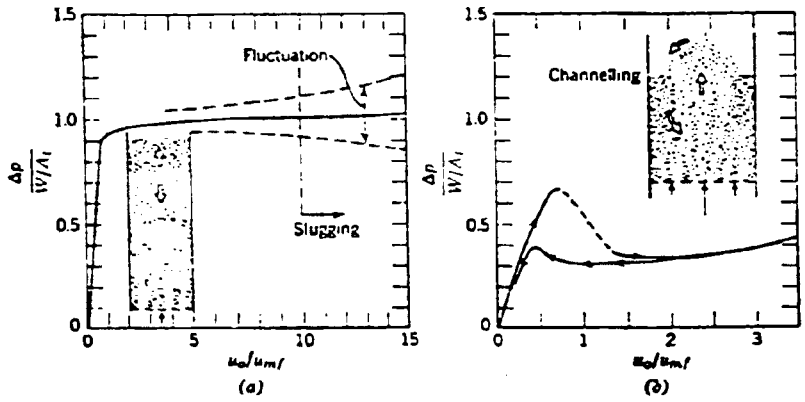

Figure III-2 Pressure Drop Behavior in an Abnormal Fluidized Bed

Although technically the foregoing arguments are valid only for two phase fluidized beds, Dakshinamurty et al [2] have shown that at atmospheric pressure and low superficial gas velocities of less than 1 cm/sec, the presence of the third (gas) phase has little effect on the bed expansion behavior.

2. Experimental Program

The actual experimental program was divided into two parts:

- Low Pressure Fluidization
- High Pressure Fluidization

Little work at all has been done on three phase flow systems at atmospheric conditions (see Section III-D) much less at elevated temperatures and pressures. There is no reason to believe, a priori, that the high pressure system would behave identically to the atmospheric case. The purpose of this work is to evaluate the behavior of a three phase fluidization system at elevated temperatures and pressure and to correlate the systems' behavior at the above mentioned conditions with the behavior at ambient temperatures and pressure.

B. Low Pressure Glass Unit

1. Experimental Apparatus

A schematic diagram of the experimental unit is given in Figure III-3. This fluidization unit consists of a catalyst filled glass tube with independent gas (CO_2) and liquid (water and hexane) flows. The 7/8" diameter tube was fitted with two 50 mesh screens about 20 inches apart; the top screen prevents catalyst carryover while the bottom screen serves as the catalyst support. The liquid stream is admitted several inches below the support screen and mixes with the gas at the sparger, which is centered directly beneath the screen. An external scale is used to determine bed expansion ratios as a function of the liquid and gas flows. In addition, system pressure drop and pressure drop above the no-solids case are also noted along with a general description of the fluidized bed activity.

2. Results

Three systems were investigated in this unit:

a) Hexane - CO_2 - 1/16" Catalyst Extrusions (1/16" - 1/8" long)
b) Hexane - CO_2 - 1/16" Catalyst Extrusions (1/16" - 1/4" long)
c) Water - CO_2 - 1/16" Catalyst Extrusions (1/16" - 1/4" long)

Figure III.3 . Schematic Diagram of the Atmospheric Pressure Liquid-Gas- Solid Fluidized Bed

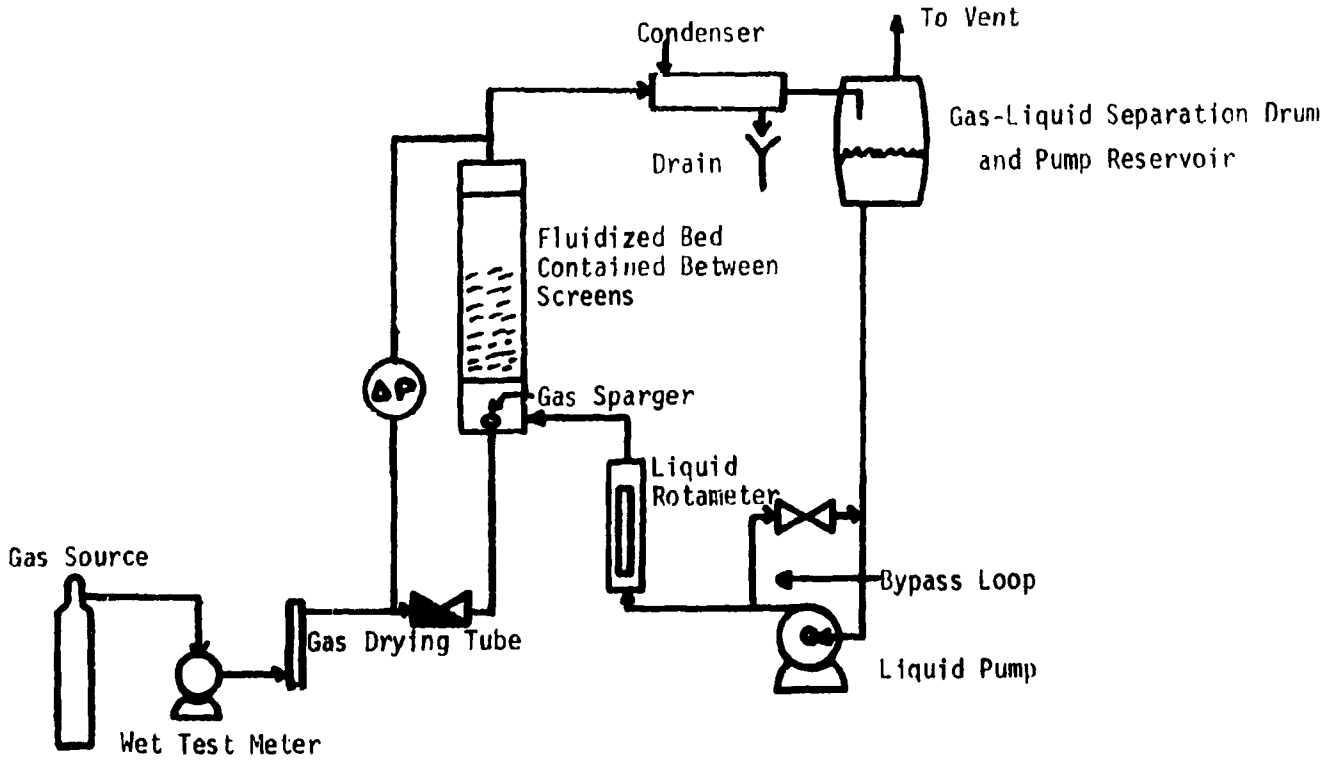

Table III-1

Bed Expansion Ratios in Three Phase Flow

Hexane/CO_2

Run No. 46-1

Catalyst Loading: 70.5 grs

H_{mf}: 13.5 cm

d_p : 0.208 cm

ρ_s : 3.7 gr/cm^3

ϕ_s : 0.859

Liquid Flow Gal/Min-Ft^2	Gas Flow Liters/Hour	H/H_{mf}
0	0	1.00
0	45	0.98
0	95	1.02
0	160	1.10
26.4	0	1.02
26.4	45	1.06
26.4	95	1.07
26.4	160	1.15
35.1	45	1.02
43.9	0	1.02
65.5	0	1.17
65.5	45	1.25
65.5	95	1.33
65.5	160	1.50
88.0	0	1.34
88.0	45	1.42
88.0	95	1.51
88.0	160	1.84
110.2	0	1.55
110.2	45	1.63

Run No. 46-9

Catalyst Loading: 58.1 grs

H_{mf}: 12.4 cm

d_p : 0.247 cm

ρ_s : 3.7 gr/cm^3

ϕ_s : 0.806

Liquid Flow Gal/Min-Ft^2	Gas Flow Liters/Hour	H/H_{mf}
0	40	1.00
0	105	1.00
0	170	1.03
18.4	170	1.02
36.0	105	1.00
41.6	40	1.00
66.4	40	1.12
66.4	105	1.23
66.4	170	1.35
105.6	40	1.39
105.6	105	1.56

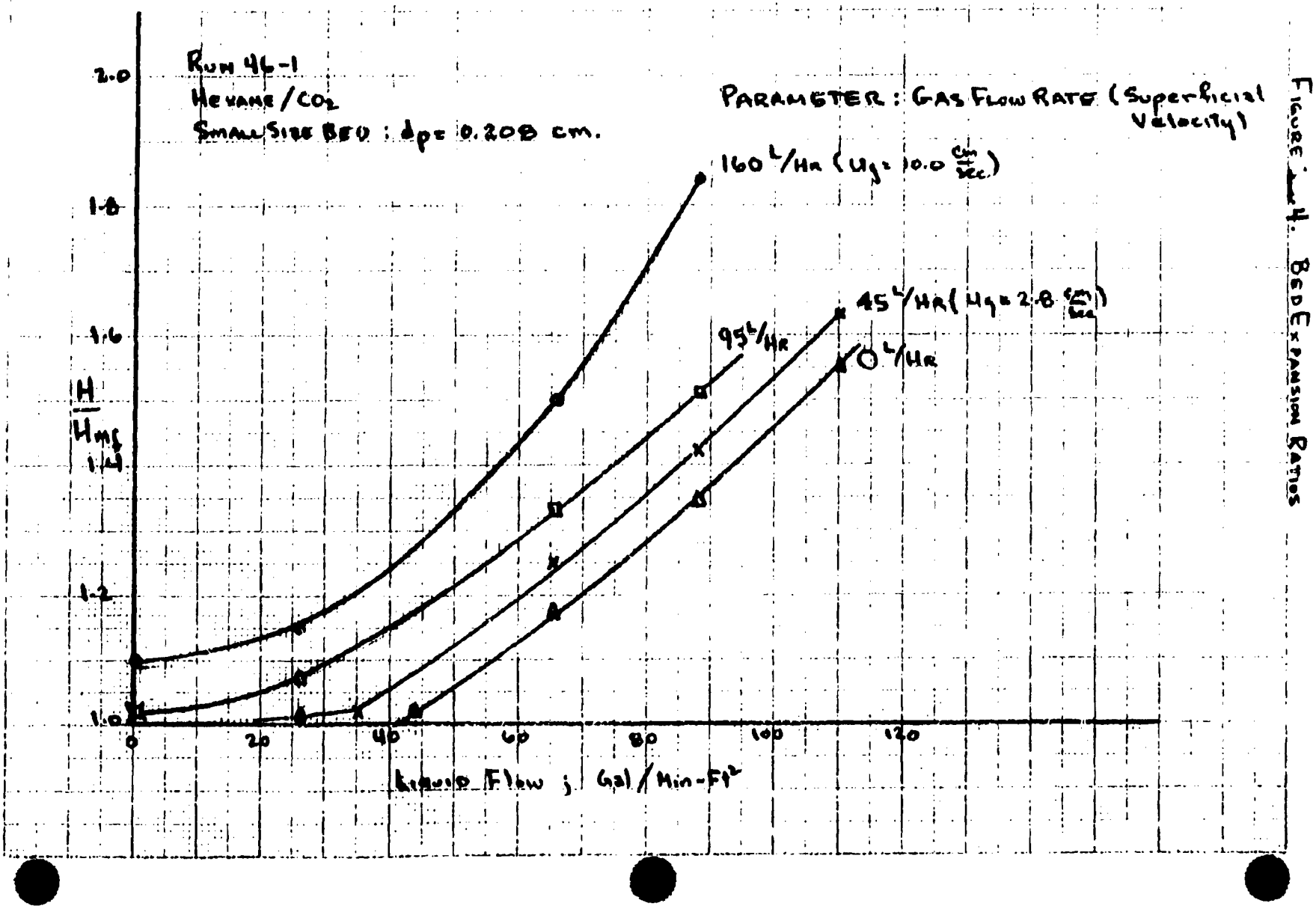

Figure 4. Bed Expansion Ratios

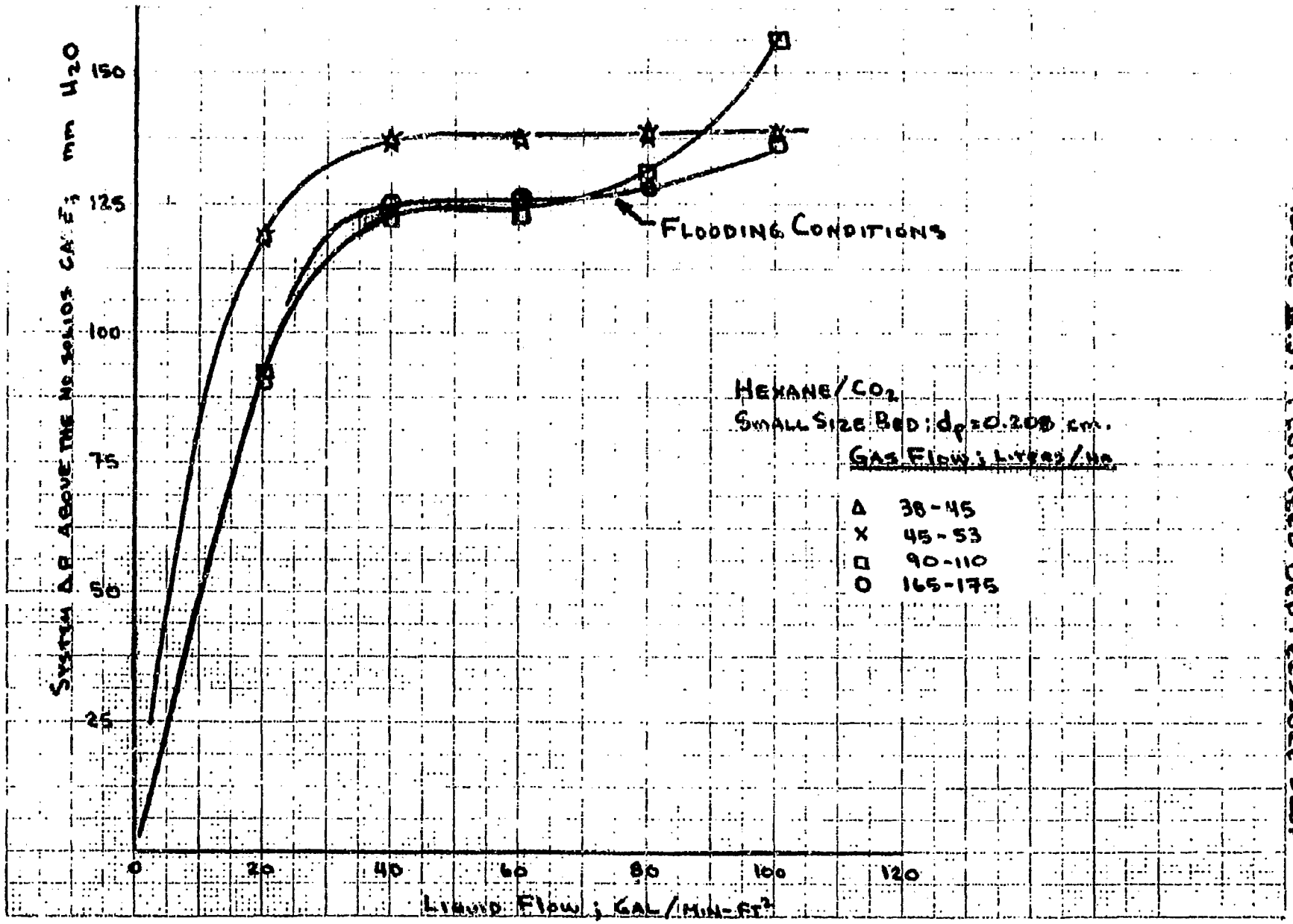

Figure II.5. Fluidized Bed Pressure Drop

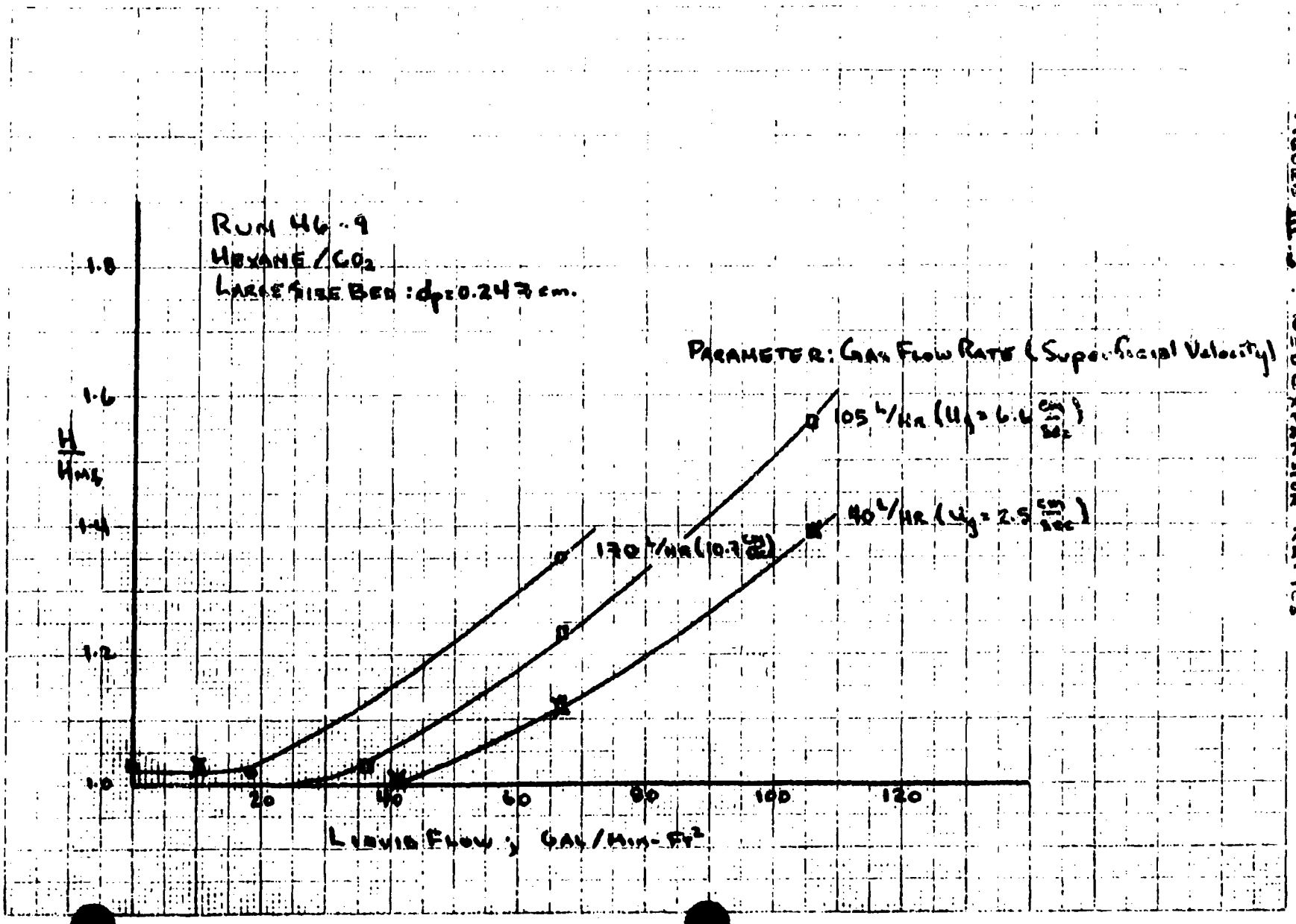

FIGURE III-8. BED EXPANSION RATIO

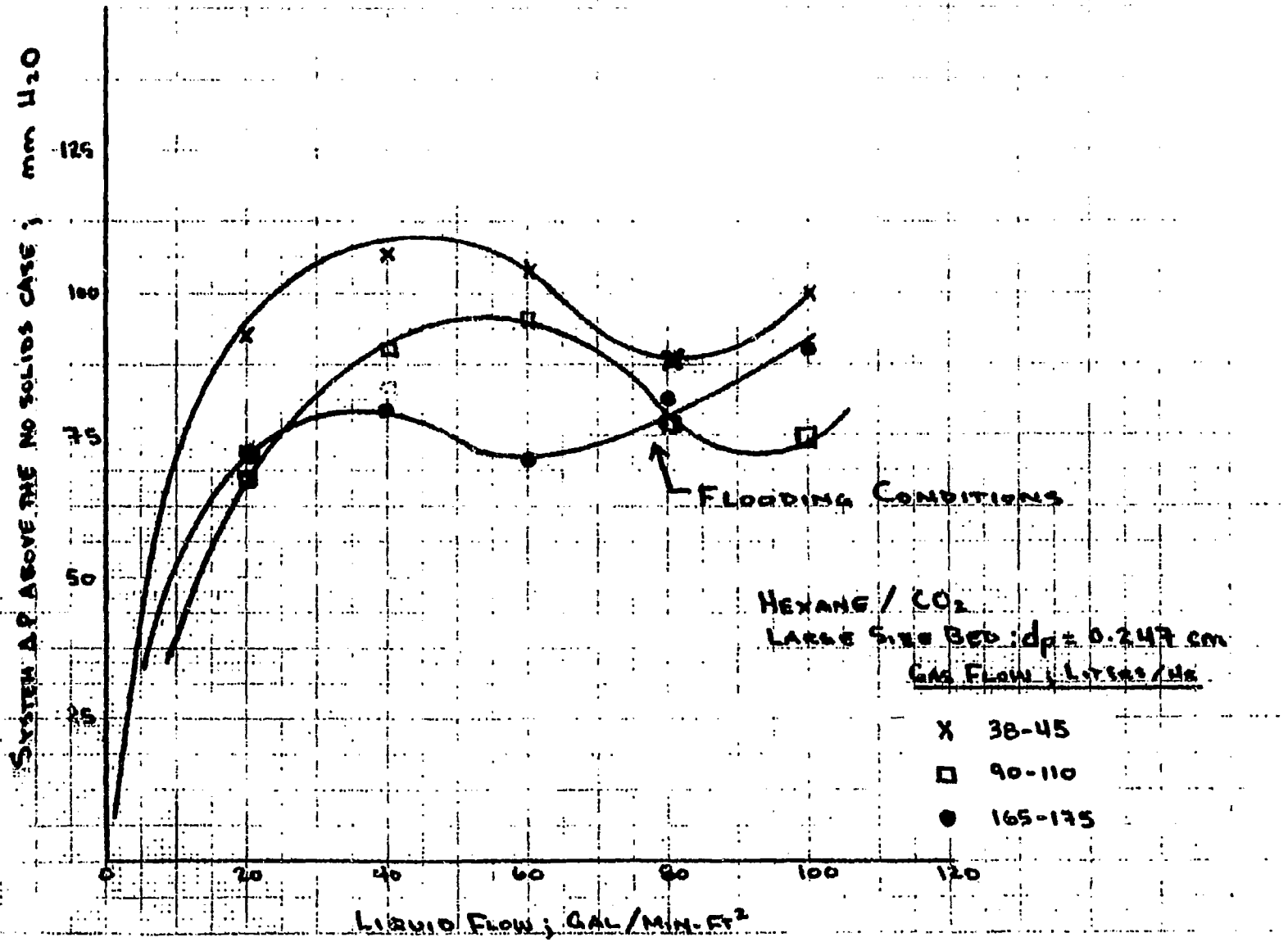

FIGURE 7. FLUIDIZED BED PRESSURE DROP

Table II-2

Bed Expansion Ratios in Three Phase Fluidized Beds

Water/CO_2

Run No. 46-10

Catalyst Loading: 58.1 grs

H_{mf}: 12.4 cm

d_p : 0.247 cm

ρ_s : 3.7 gr/cm^3

$\emptyset_s$: 0.806

Liquid Flow Gal/Min-Ft^2	Gas Flow Liters/Hour	H/H_{mf}
0	55	1.00
0	95	1.00
0	150	1.01
3.2	55	1.00
3.2	95	1.00
19.2	55	1.08
19.2	95	1.11
19.2	150	1.31
49.6	55	1.39
49.6	95	1.56
49.6	150	1.80
62.4	95	1.84
82.4	55	1.79

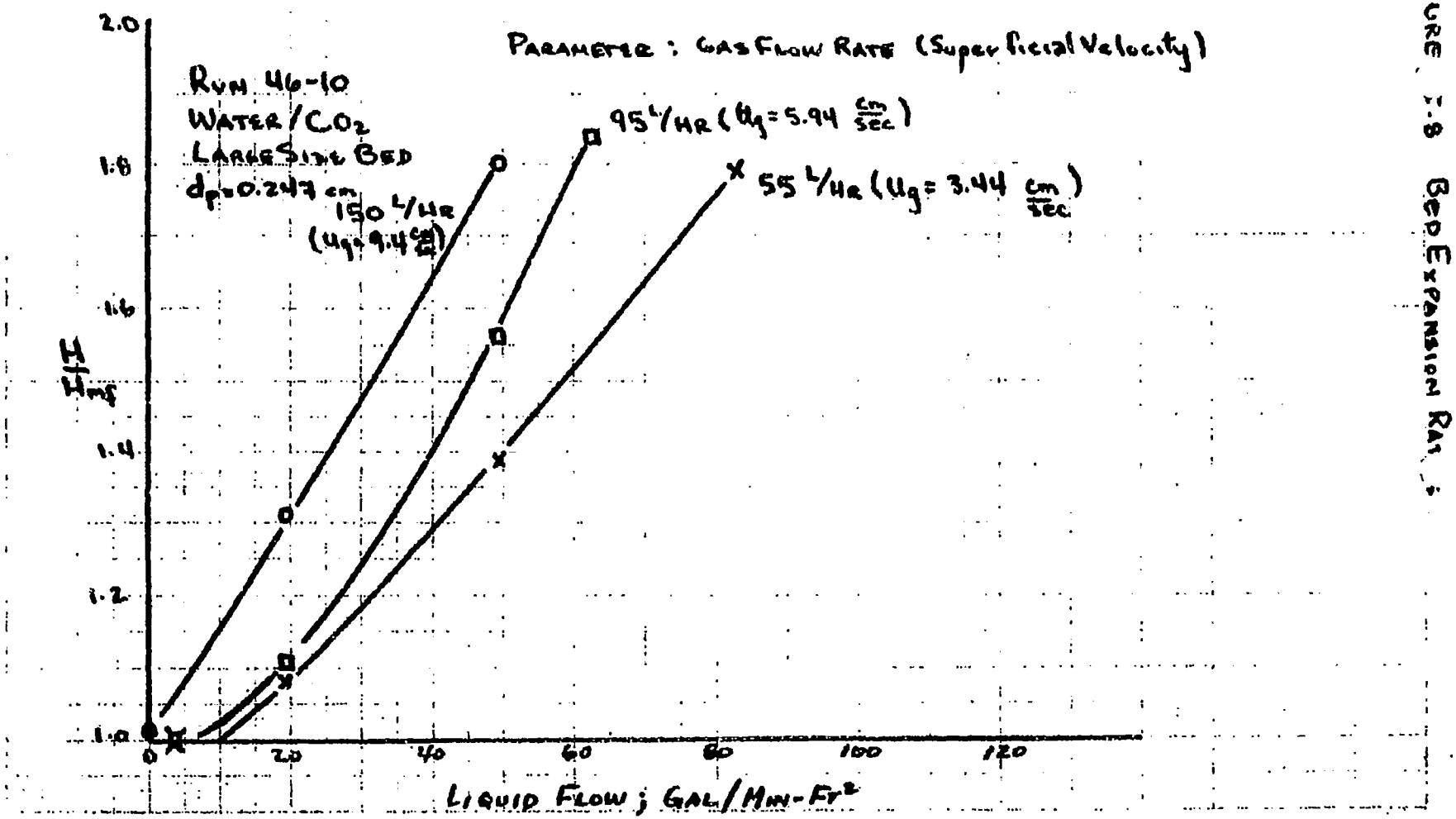

FIGURE 7.8 BED EXPANSION RA

FIGURE 9. FLUIDIZED BED PRESSURE DROP

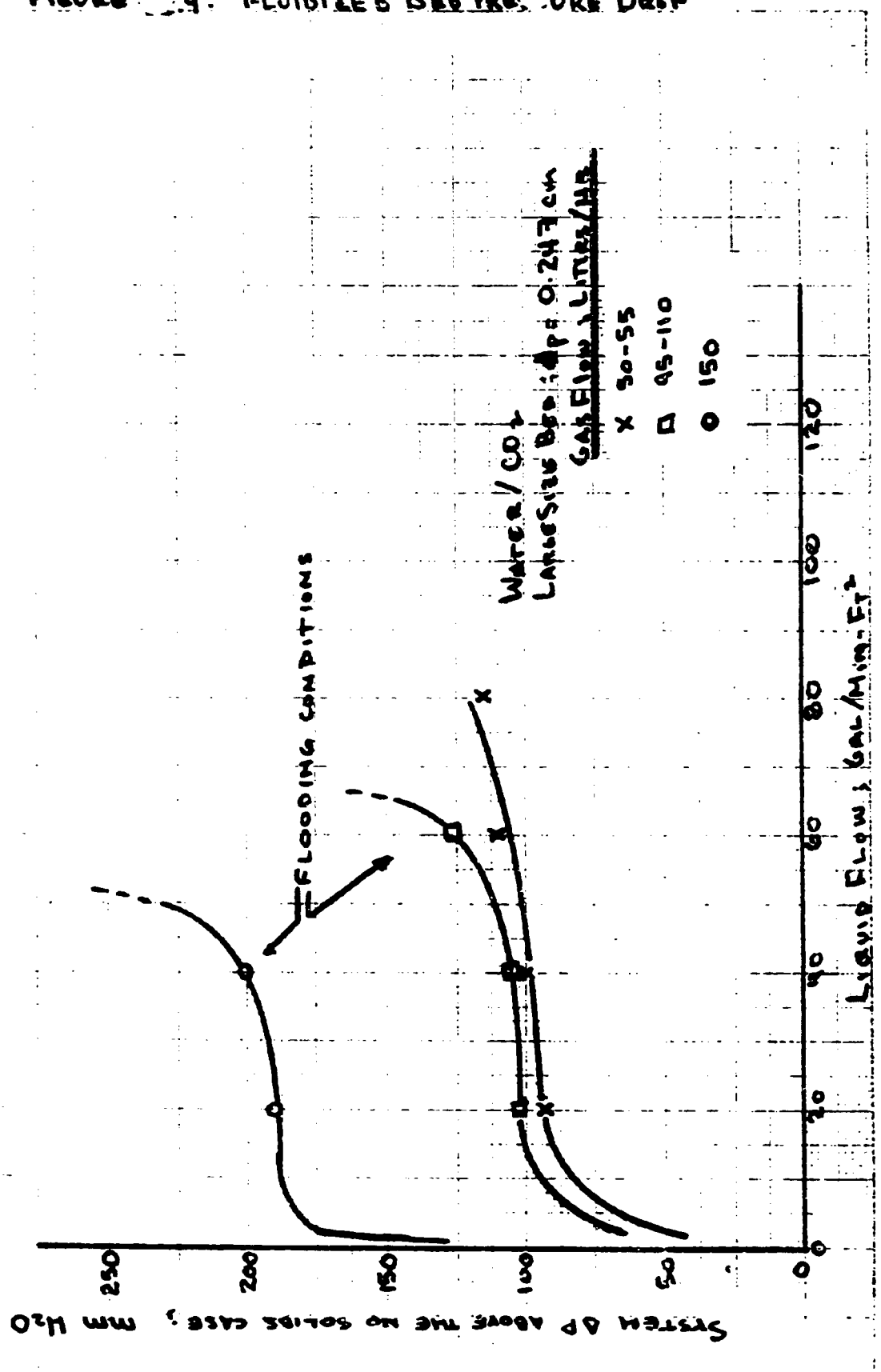

A comparison of systems a and b will correlate the effect of particle size while comparisons between systems b and c will relate to physical property differences between hexane and water. The data are presented in Tables III-1 and III-2 and Figures III-4 to III-9.

C. High Pressure Glass Unit

1. Experimental Apparatus

A schematic diagram is given in Figure III-10. In its operation, the high pressure system is quite similar to the atmospheric fluidized bed. The basic differences simply result from the complications introduced by operating at 1000 psig and 650°F. The fluidized bed was fashioned from a high pressure, high temperature sight glass fitted with a gas sparger centered below the bed support screen. Electrical heating tapes were used to control the system temperature, and hence fluid properties, while a back pressure regulator was used to adjust system pressure. Gas and liquid flow rates were individually adjusted. Because of the high system pressures, it was not possible to obtain reliable pressure drop data. This is of little consequence here since the bed is visible. In the next phase, however, accurate fluidized bed pressure drops will be a valuable tool, in fact the only tool, in detailing bed activity.

2. Results

To simplify the experimental procedure, the influence of fluid properties was investigated by varying the system temperature, using a single fluid, Dowtherm A, rather than using a single temperature with a variety of fluids. The liquid properties of interest are the density and viscosity, and at the three temperature levels used, they are shown in Table III-3.

Process Equipment List

1. Atmospheric Liquid-Gas Separation Drum with Level Indicator
2. Liquid Pump
3. Heat Exchanger
4. Oil Preheater
5. Gas Preheater
6. High Pressure Sight Glass Fluidized Bed
7. Oil-Gas Cooler
8. Back Pressure Regulator
9. Wet Test Meter
10. Solenoid Safety Valves
11. High-Low Pressure Cutoff Switch
12. Temperature Indicator
13. Temperature Recorder/Controller with Alarm Function
14. Manually Operated Rheostats

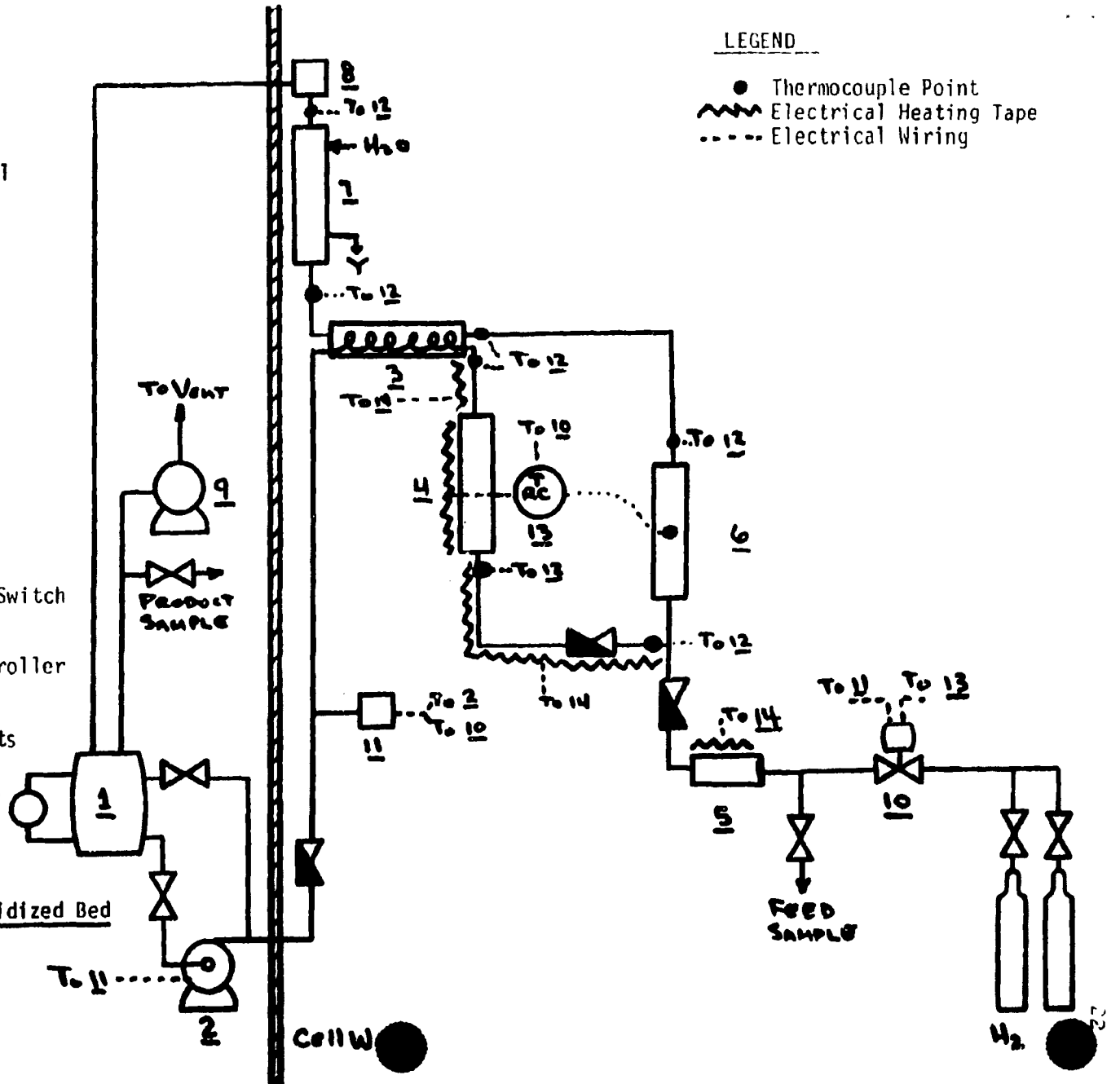

Figure III.10 .
Schematic Diagram of the High Pressure Liquid-Gas-Solid Fluidized Bed

Table III-3

Physical Properties of Dowtherm A

Temperature, ^{o}F	ρ, gr/cm^3	μ, Centipoise
335	0.939	0.5
465	0.871	0.3
630	0.774	0.18

The same catalyst was used in this experimental phase as well as in the low pressure work with the exception that it was ground to a 30-50 mesh size. The literature indicates that gas density has little effect on fluidized bed properties, and nitrogen was used as a matter of convenience. The liquid flow rates were varied up to a 25 gal/min-ft^2 while gas flows were set at approximately 500, 1500 and 2500 SCF gas-hr/CF of reactor volume. The results are given in terms of bed expansion ratios and bed voidage as a function of flow rates. At the outset it became readily apparent that the high pressures reduced the superficial gas velocities in the bed to such low levels that the gas has essentially no effect on bed expansion, though mixing patterns were still affected to a measurable extent. Gas flows, nevertheless, were adjusted at the higher temperatures to give superficial velocities similar to the $335^{o}F$ base case values of 0, 0.12, 0.36 and 0.60 cm/sec which correspond to VHSV's of 500, 1500 and 2500 respectively.

Table III-4

Bed Expansion Ratios* - Dowtherm A/N_2

335°F			465°F			630°F		
Liquid Flow l/Min-Ft^2	Gas Flow Liters/Hr	H/H_{mf}	Liquid Flow Gal/Min-Ft^2	Gas Flow Liters/Hr	H/H_{mf}	Liquid Flow Gal/Min-Ft^2	Gas Flow Liters/Hr	H/H_{mf}
8.09	0	1.18	6.4	0	1.03	6.4	0	1.00
8.09	82	1.19	6.4	80	1.05	6.4	60	1.00
8.09	265	1.17	6.4	220	1.06	6.4	178	1.01
8.09	415	1.16	6.4	365	1.06	6.4	300	1.01
14.4	0	1.26	12.6	0	1.17	12.6	0	1.13
14.4	86	1.27	12.6	70	1.18	12.6	60	1.13
14.4	250	1.26	12.6	225	1.17	12.6	182	1.13
14.4	410	1.25	12.6	370	1.18	12.6	297	1.13
20.2	0	1.50	19.3	0	1.27	19.3	0	1.22
20.2	87	1.50	19.3	75	1.25	19.3	62	[illegible]
6.3	0	1.10	19.3	230	1.27	19.3	182	[illegible]
6.3	88	1.12	19.3	400	1.27	19.3	310	1.23
6.3	248	1.10	25.3	0	1.41	25.3	0	1.32
6.3	440	1.10	25.3	72	1.41	25.3	60	1.34
19.3	0	1.41	25.3	220	1.41	25.3	175	1.32
19.3	87	1.41	25.3	398	1.41	25.3	315	1.32
19.3	255	1.45	25.3					
19.3	405	1.45						
25.4	0	1.65						
25.4	87	1.67						
25.4	240	1.69						
25.4	430	1.67						
6.4	0	1.12						
12.1	0	1.27						
6.8	0	1.44						
25.3	0	1.70						

H_{mf} : 126 mm
d_p : 0.045 cm
ρ_s : 3.7 gr/cm^3
$\emptyset_s$: 0.67

At gas flows greater than 200 liters/hour, values given for the bed expansion ratio represent the mean of the fluctuating bed height.

FIGURE III.11. BED EXPANSION RATIOS*

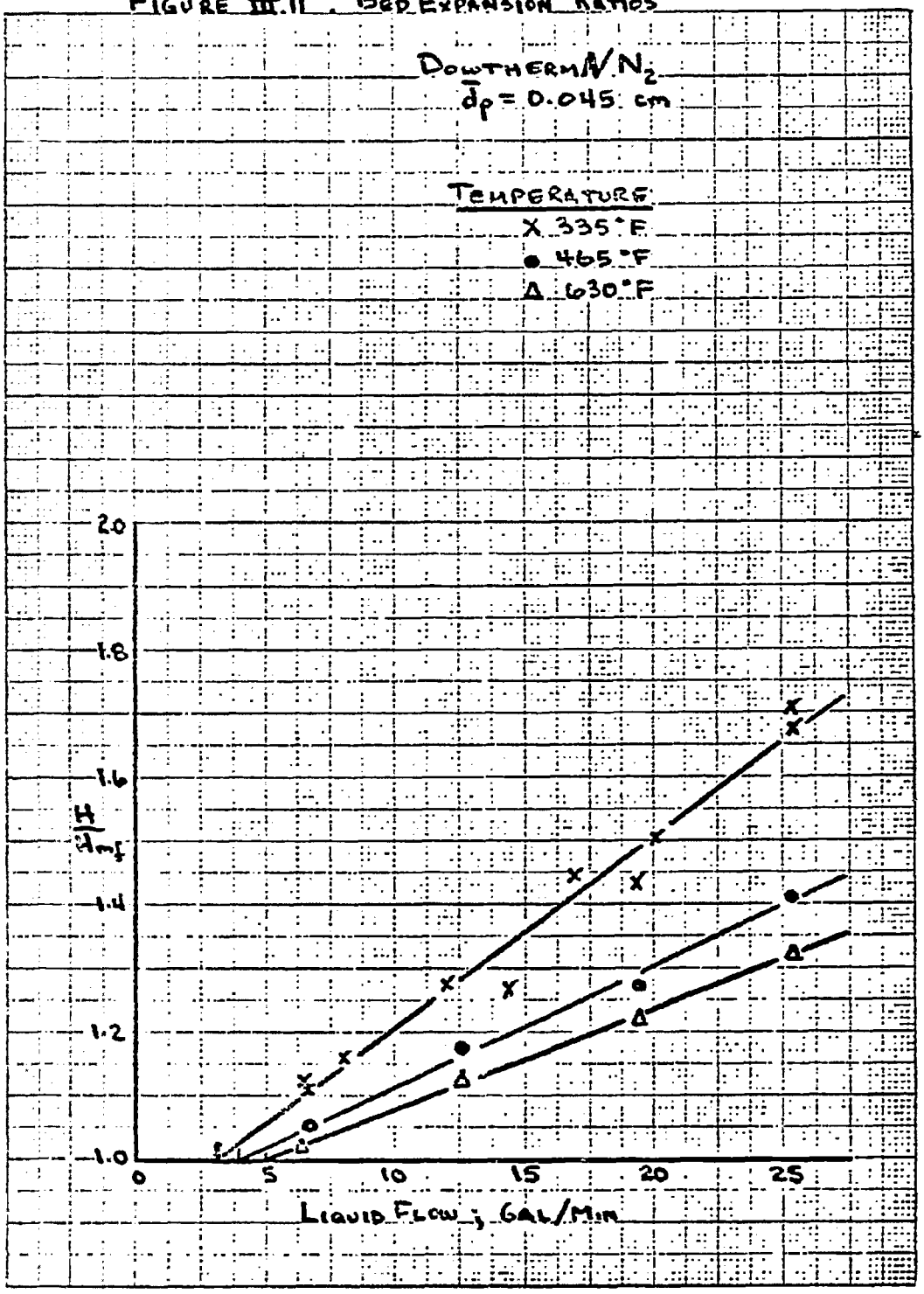

* AVERAGE VALUES FOR ALL GAS FLOWS.

Table III-5

Bed Porosity* - Dowtherm A/N_2

335°F		465°F		630°F	
Liquid Flow Gal/Min-Ft^2	ϵ	Liquid Flow Gal/Min-Ft^2	ϵ	Liquid Flow Gal/Min-Ft^2	ϵ
6.3	0.536	6.4	0.514	6.4	0.495
6.4	0.545	12.6	0.566	12.6	0.549
8.09	0.564	19.3	0.605	19.3	0.584
12.1	0.598	25.3	0.638	25.3	0.614
14.4	0.595				
16.8	0.646				
19.3	0.643				
20.2	0.660				
25.3	0.700				
25.4	0.695				

*Based on $\epsilon_{mf} = 0.49$

FIGURE III.12 BED POROSITY : DOWTHERM A/N_2

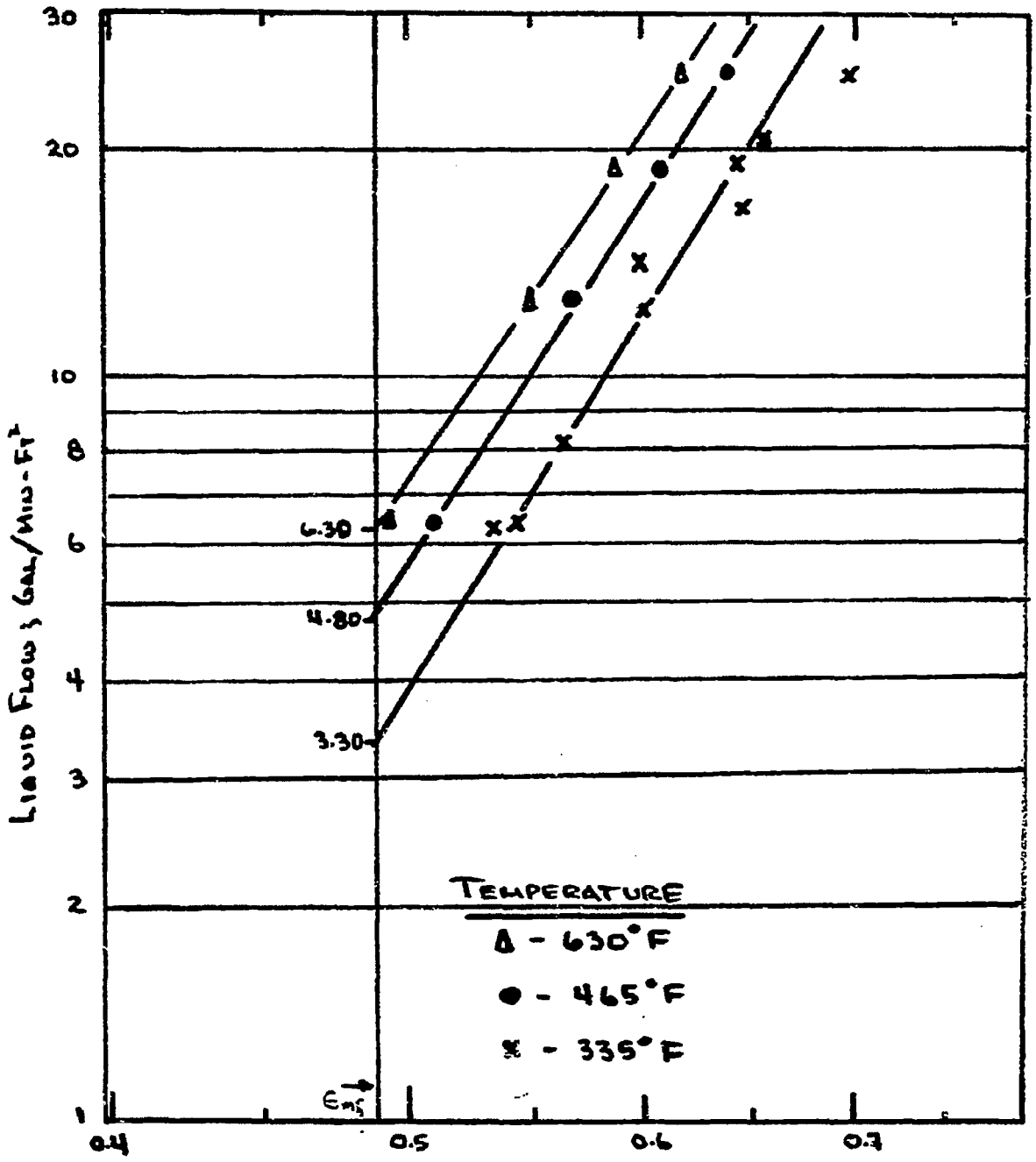

ϵ_{mf} = 0.49 FOR 30-50 MESH G-65 RS CATALYST

D. Results Obtained By Other Investigators

Little work has been done on three phase fluidized beds. Of interest to us are two studies; one by R. Wolk [3], the other by Dakshinamurty and coworkers [2]. Wolk used the systems water/nitrogen and hexane/nitrogen with various size cylindrical particles (3/16" long with diameters of 0.025", 0.050" and 0.0625"). He also investigated the effect on tube diameter over the range of 1.00" to 6.00". His data could be correlated in the form:

$$D = A - F_1 F_2 \qquad (6)$$

where:

D = Bulk bed density
A = Bulk bed density with liquid flow only (independent of tube diameter)
F_1 = Correction factor for gas flow (function of tube diameter)
F_2 = Secondary correction factor for the effect of liquid flow on F_1

Typical results are shown for the 0.0625" diameter extrudates hexane/nitrogen system in Figures III-13 and III-14. If we were to superimpose our small size particle low pressure data, we would find all our points shifted to the right by about 20 gal/min-ft^2, but the curves would have the identical form. This is further discussed in Section IV and shown in Figure IV-2. Wolk further analyzed his data in terms of the "net" liquid velocity, equivalent to the superficial liquid velocity divided by the volume fraction of liquid, which he considers to be the effective force for fluidization. In this manner he was able to correlate his data independent of tube diameter, as in Figure III-15.

Limited data with a variety of fluids and solids was obtained by Dakshinamurty et al. In an attempt to ascertain the effects of liquid viscosity and surface tension and particle density on bed expansion, these authors also investigated the effect of liquid and gas flow on fluidization behavior. Their data

IGURE III.13

FIGURE 4

EXPANSION OF THE 0.063 INCH CYLINDRICAL EXTRUDATE WITH HEPTANE AND NITROGEN IN A 1.00 INCH ID TUBE (3)

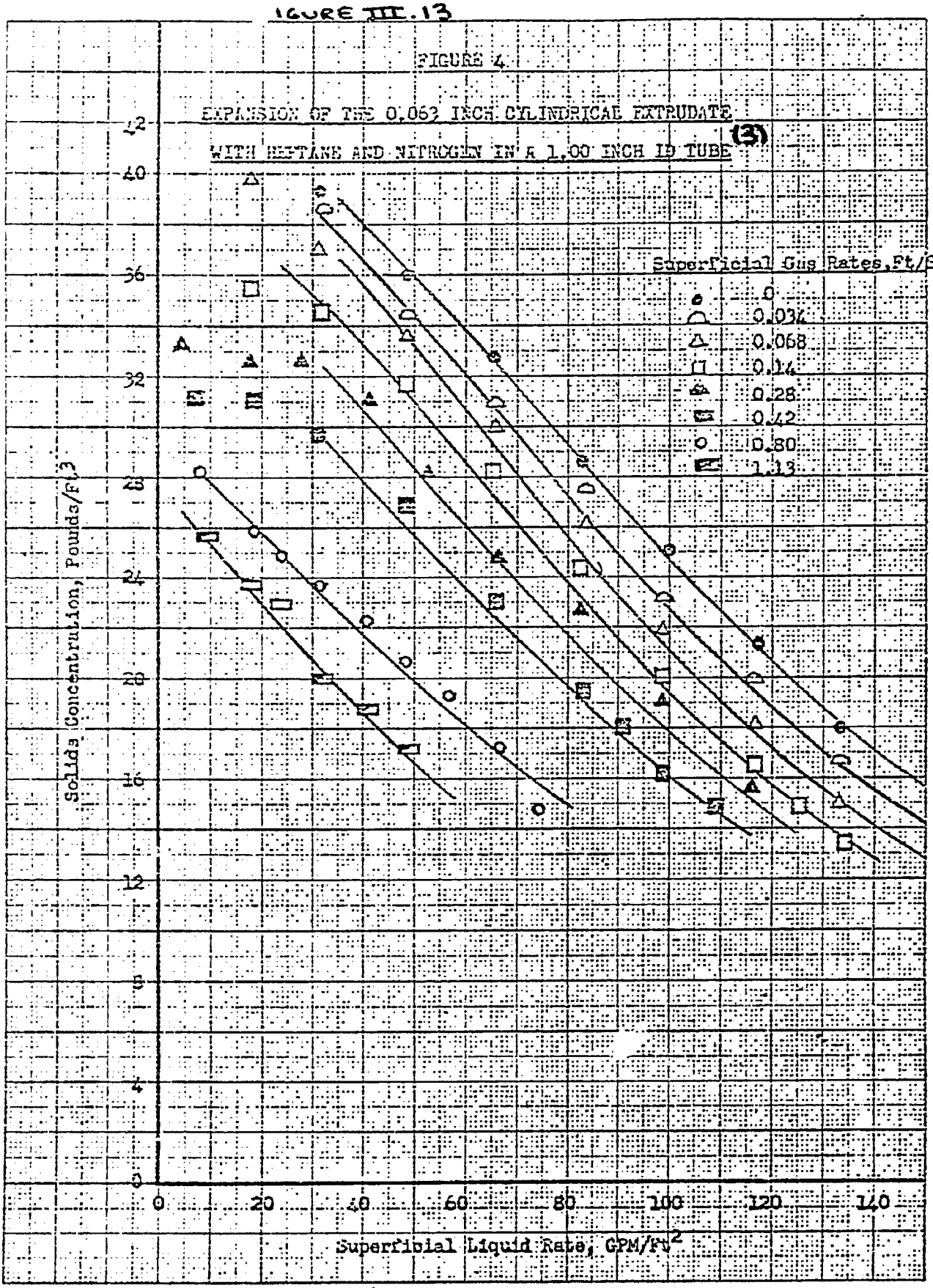

FIGURE III.14

FIGURE 8

SOLIDS CONCENTRATION "D", POUNDS/FT^3 FOR 0.063" SOLIDS IN VARIOUS TURBS WITH HEPTANE AND NITROGEN (3)

$$D = A - F_1 F_2$$

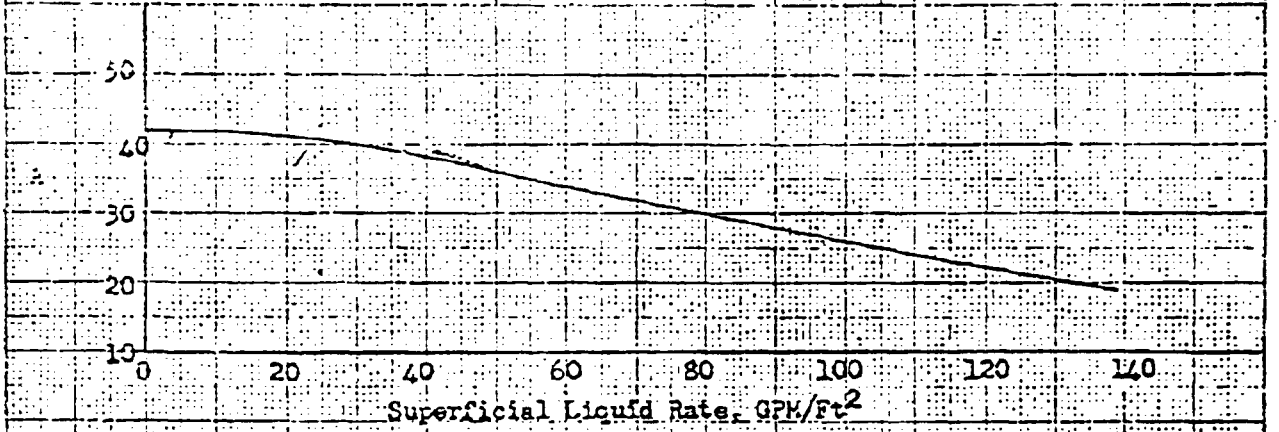

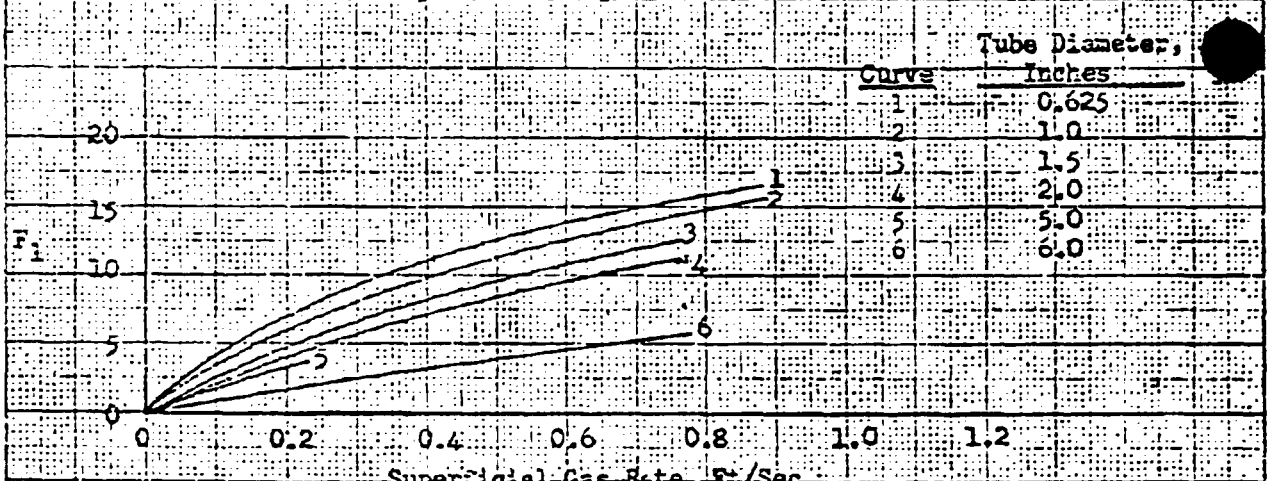

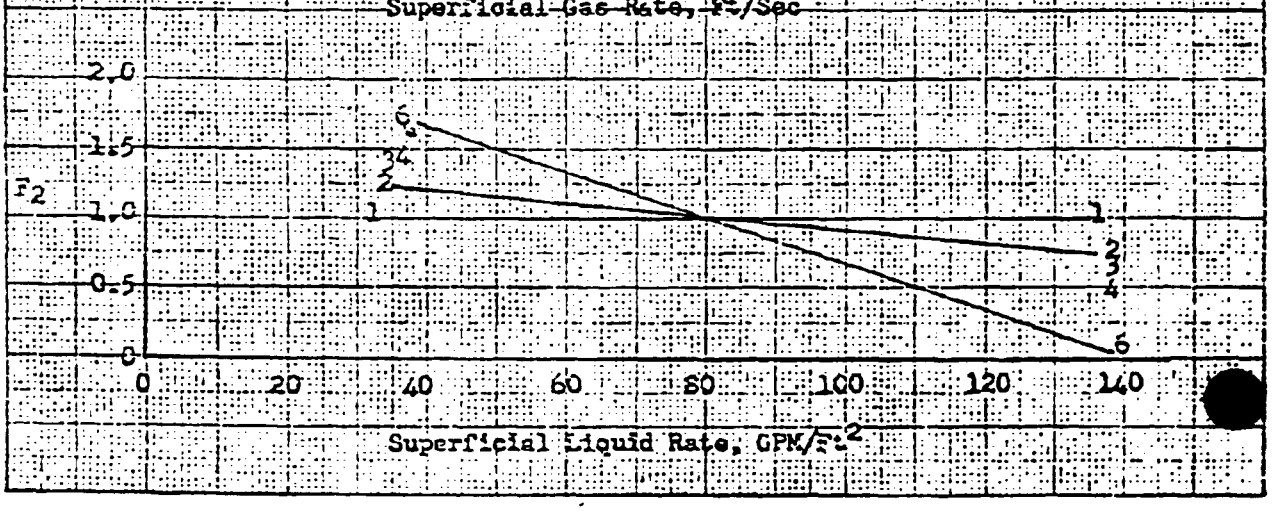

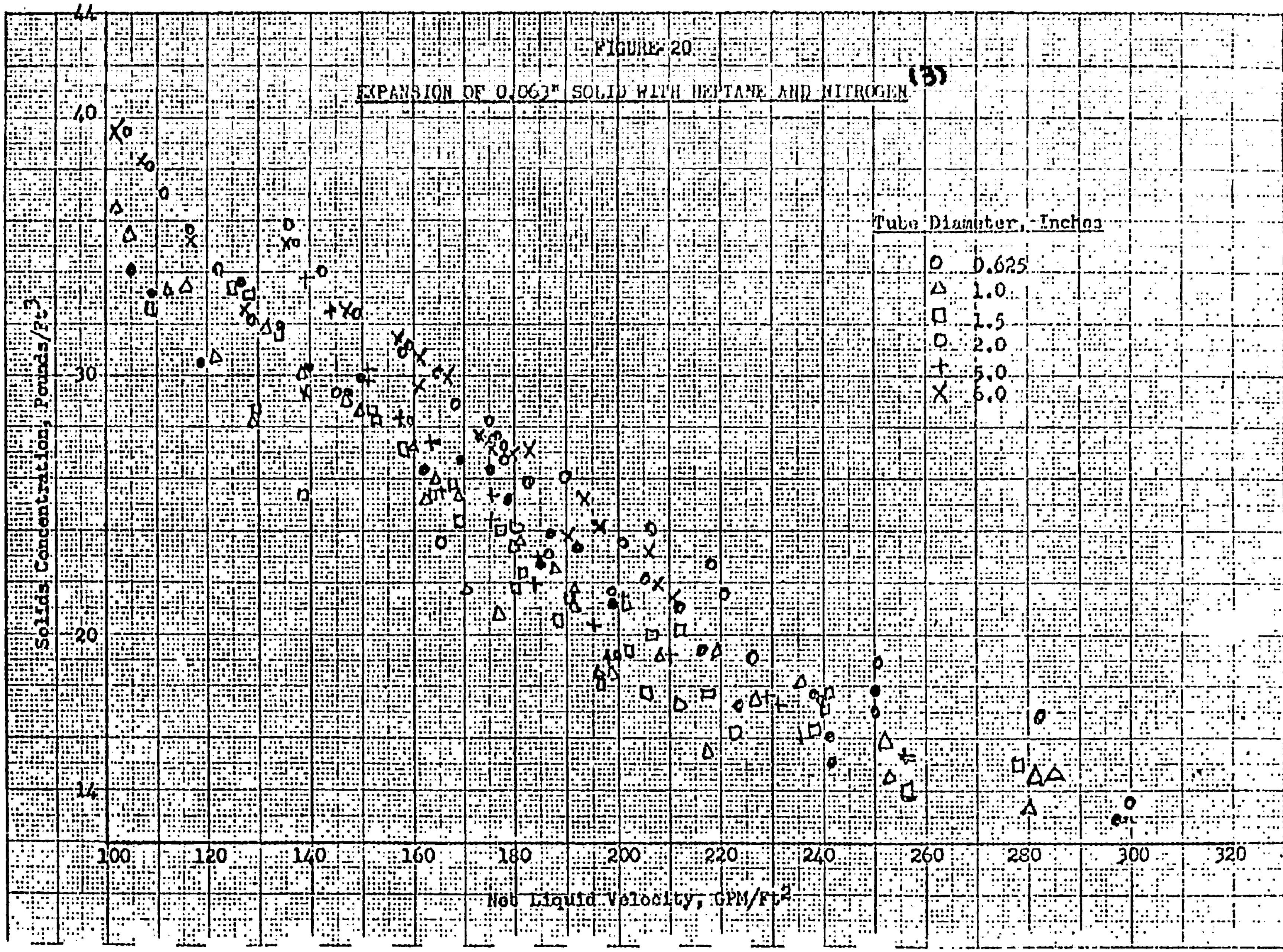
FIGURE 20
EXPANSION OF 0.063" SOLID WITH HEPTANE AND NITROGEN
(3)
Tube Diameter, Inches
0.625
1.0
1.5
2.0
5.0
6.0
Solids Concentration, Pounds/Ft³
44
40
30
20
14
100
120
140
160
180
200
220
240
260
280
300
320
Net Liquid Velocity, GPM/Ft²
est

FIG 3E III.15

could be correlated by the following expressions:

$$\epsilon = 2.65\left(\frac{u_l}{u_t}\right)^{0.6}\left(\frac{\mu_l\, u_g}{\sigma_l}\right)^{0.08} \qquad Re_t > 500$$

$$\epsilon = 2.12\left(\frac{u_l}{u_t}\right)^{0.41}\left(\frac{\mu_l\, u_g}{\sigma_l}\right)^{0.08} \qquad Re_t < 500 \qquad (7)$$

The basic shortcoming of the above relationship is the inability to predict voidage at gas velocities approaching zero. Interesting enough, at gas velocities below 1 cm/sec, they observed a contraction of the bed when compared with a similar bed without gas flow. This contraction is small, 10% at most, and is most prominent with small particles at gas velocities of about 0.5 cm/sec. They attribute the contraction to an overall lowering of the superficial liquid velocity caused by the high local liquid velocity in the wake of a coalescing gas bubble. It should be noted that bubble coalescence is substantial in beds having a low expansion ratio. Typical data are shown for the systems kerosine/air/glass beads and water/air/glass beads in Figure III-16. It is readily apparent that these systems are much more sensitive to liquid velocity than ours; this might be due to the substantially different particle geometry used, where theirs are uniform spherical beads while ours are irregularly shaped particles with a wide size distribution.

FIGURE III.16 . BED POROSITY VS. GAS FLOW RATE; LIQUID FLOW RATE AS A PARAMETER

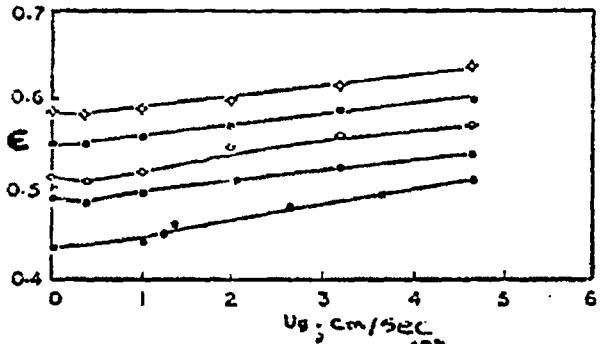

Figure 5. ε vs. U_g plot[2]

System: small glass beads -air-water

9.0 8.0 7.2 6.65 6.10

U_l ; cm/sec

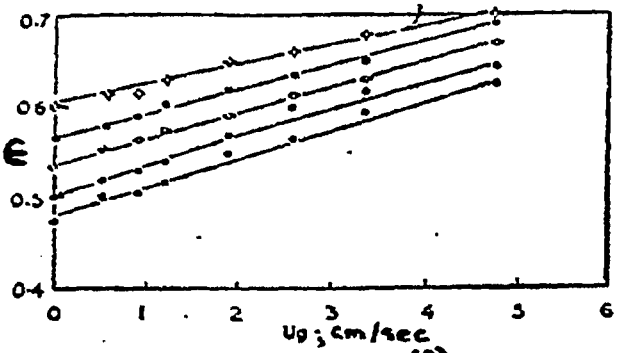

Figure 6. ε vs. U_g plot[2]

System: small glass beads air-kerosine

10.6 9.46 8.44 7.65 6.75

U_l ; cm/sec

IV DISCUSSION OF RESULTS

A. Introduction

As a basis for comparison of our results, we have chosen both the theoretical approach as outlined in Section III and the experimental results of others who have examined similar systems. The first goal is to evaluate our results by comparing them with the data generated by others in addition to developing the basis for a model that will enable us to predict fluidization behavior from our knowledge of gas and liquid flow.

B. Fluidization Results

It is apparent that superficial gas velocities less than 0.6 cm/sec have no measurable effect on bed expansion and it will therefore be more instructive to consider the results in two parts; low gas flow rates ($\lesssim$0.6 cm/sec) and high gas flow rates. The low gas flow rate data include part of the Low Pressure Unit data and all of the High Pressure Unit data. The high gas flow data were generated in the Low Pressure Unit.

1. Low Gas Superficial Velocities

The theoretical analyses presented in Section III apply rigorously only to two-phase fluidization. However, as we have already pointed out, superficial gas velocities less than 0.6 cm/sec have little effect on bed expansion behavior and comparisons between experimental three-phase fluidization and predicted fluidization behavior for a two-phase system will still be instructive.

Table IV-1 provides a description of the solid phase materials while Table IV-2 presents the conditions of the experiments, tabulating the actual results along with the predicted values. In all cases, the actual

Table IV-2

Analyses of Fluidization Results

Low Pressure Unit

System	μ_L; Poise	ρ_L; gm/cm^3	Particle Size	Actual u_{mf} cm/sec	Theoretical u_{mf}; cm/sec	Actual ΔP_{mf}; mm H_2O	Theoretical ΔP_{mf}; mm H_2O
Water/CO_2	0.009	1.0	1/16" Diam. x 1/16"-1/4"	-	4.47	100	180
Hexane/CO_2	0.003	0.655	1/16" Diam. x 1/16"-1/4"	-	6.59	110	205
Hexane/CO_2	0.003	0.655	1/16" Diam. x 1/16"-1/8"	2.82	5.49	140	240

High Pressure Unit

Dowtherm A/N_2	0.005	0.939	.012 - .024"	0.224	0.692		
Dowtherm A/N_2	0.003	0.871	.012 - .024"	0.326	1.065		
Dowtherm A/N_2	0.0018	0.774	.012 - .024"	0.428	1.533		

BLANK PAGE

fluidization velocities are substantially less than the predicted values. For the most part, this is due to the inability of the theoretical analysis to account for the wide particle size distribution of the solid used in our experiments. For small particles, the minimum fluidization velocity is proportional to the square of the equivalent particle diameter. With the 30-50 mesh particles, this amounts to a four-fold variation in fluidization velocity. For large particles, minimum fluidization velocity is proportional only to the square root of the equivalent particle diameter. This smaller dependence of fluidization velocity on particle size might account for the smaller relative difference between the theoretical and experimental results obtained with these particles. Other factors might also be responsible for the variance between experimentally determined values and those predicted from the literature. Wall effects are possible with particles which are large compared to the tube diameter, and more importantly, in the high pressure reactor system, heat losses to the atmosphere from the sight glass cause radial temperature profiles and thus local increases in fluid viscosity and density which lower the liquid flow rate necessary for fluidization. As a result, fluidization is more pronounced near the walls than at the center of the chamber.

Because of the above discussed wall and thermal gradient effects, the experimental data are different from the values predicted in the literature. It is, however, clear that the observed relative behavior is in agreement with both the behavior predicted by correlations and with the system behavior observed by other investigators.

Our ultimate goal in the fluidization study is to develop an understanding, both qualitative and quantitative, of the system as to permit us to predict accurately the behavior of the three-phase system. The first step in this direction is to reduce the experimental data to an expression common to a variety of liquids, gases and flow conditions. This correlation

is given in Figure IV-1 and by the expression below. One should note that the data presented in Figure IV-1 are the same data given in Figure III-12 but reduced to more basic independent variables.

$$\epsilon = 1.144 \left(\frac{u}{u_t}\right)^{0.16} \qquad 0.49 \leq \epsilon \leq 0.70 \qquad (8)$$

u_t = Particle Terminal Velocity[4]

The power dependency on the liquid flow rate is similar to that obtained by Wolk [3] for 1/16" extrudates, but lower than that obtained by Dakshinamurty et al [2] and Hamilton [5] who obtained values of about 0.4 for uniform spherical particles.

One additional aspect of the experimental results is that the observed pressure drops are in accordance with the values predicted by the literature (as shown by equation 2 in Section III) if one uses the observed fluidization velocities rather than those predicted by the expressions for minimum fluidization. In addition, note that in Figures III-5, III-7 and III-9, the behavior is identical to that described in the literature as represented by Figure III-1. The only exception is the rise in pressure at the higher liquid flow rates, which was due solely to flooding above the liquid outlet.

2. High Gas Superficial Velocity

Our results for the high superficial gas velocity experiments are compared to the work of Wolk [3] in Figure IV-2. Note the strong similarity in expansion behavior. If the data were replotted to examine for the effect of gas velocity on bed expansion, at constant liquid flow, one would find, for the results of Wolk, that ϵ is proportional to $u_g^{0.06}$. In comparison our results show a somewhat greater dependence with a value of 0.085. Dakshinamurty et al [2] found for a variety of liquid-gas-solid systems, a value of 0.08 for the gas velocity power dependence. At the low gas velocities expected in the methanation reactor, the bed voidage, ϵ, will be increased by only about 8% at the highest gas flows.

FIGURE IV.1 REDUCED FLUIDIZATION VELOCITY VS. POROSITY

DOWTHERM A / N_2

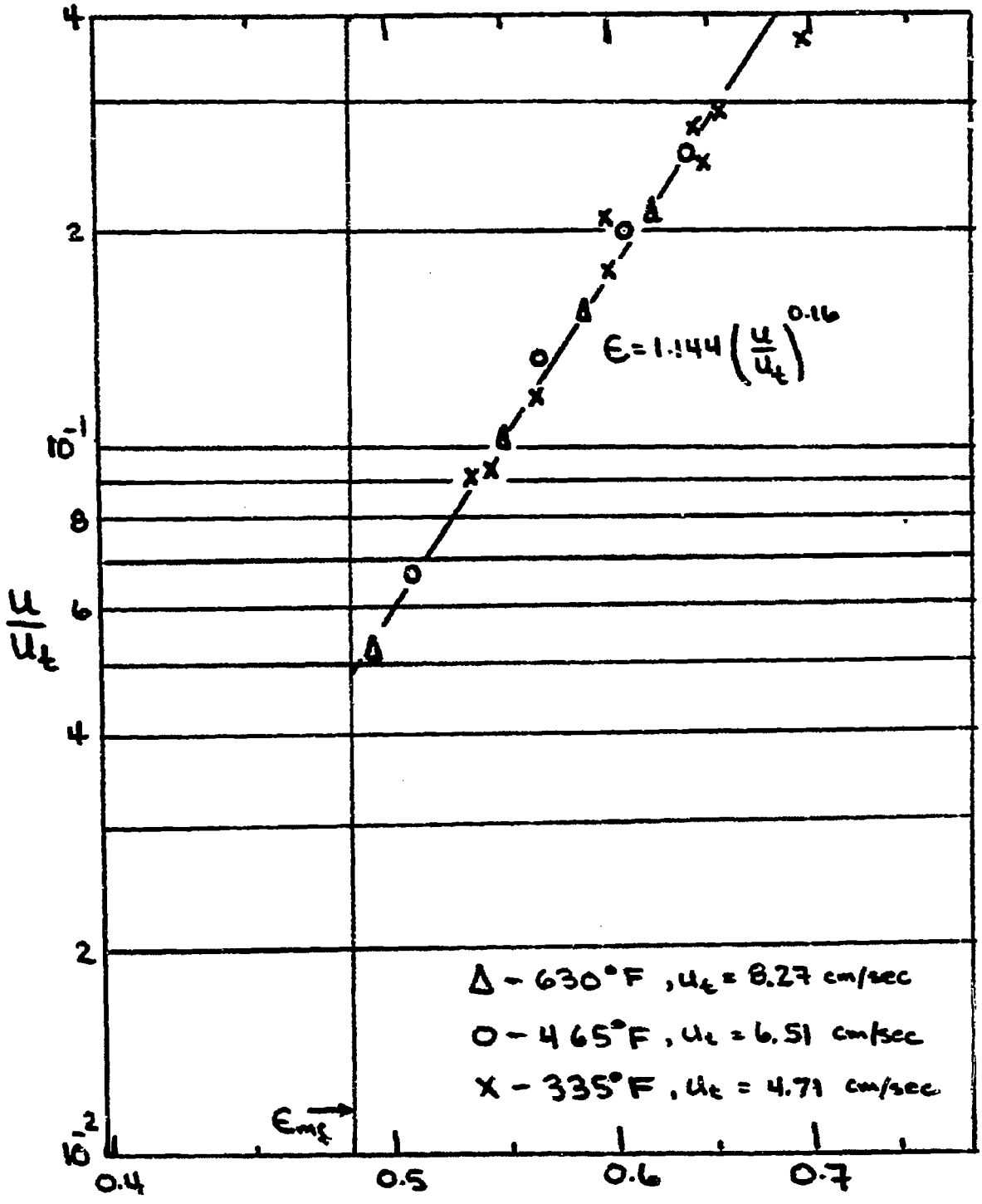

FIGURE IV.2. EFFECT OF GAS VELOCITY ON BED EXPANSION

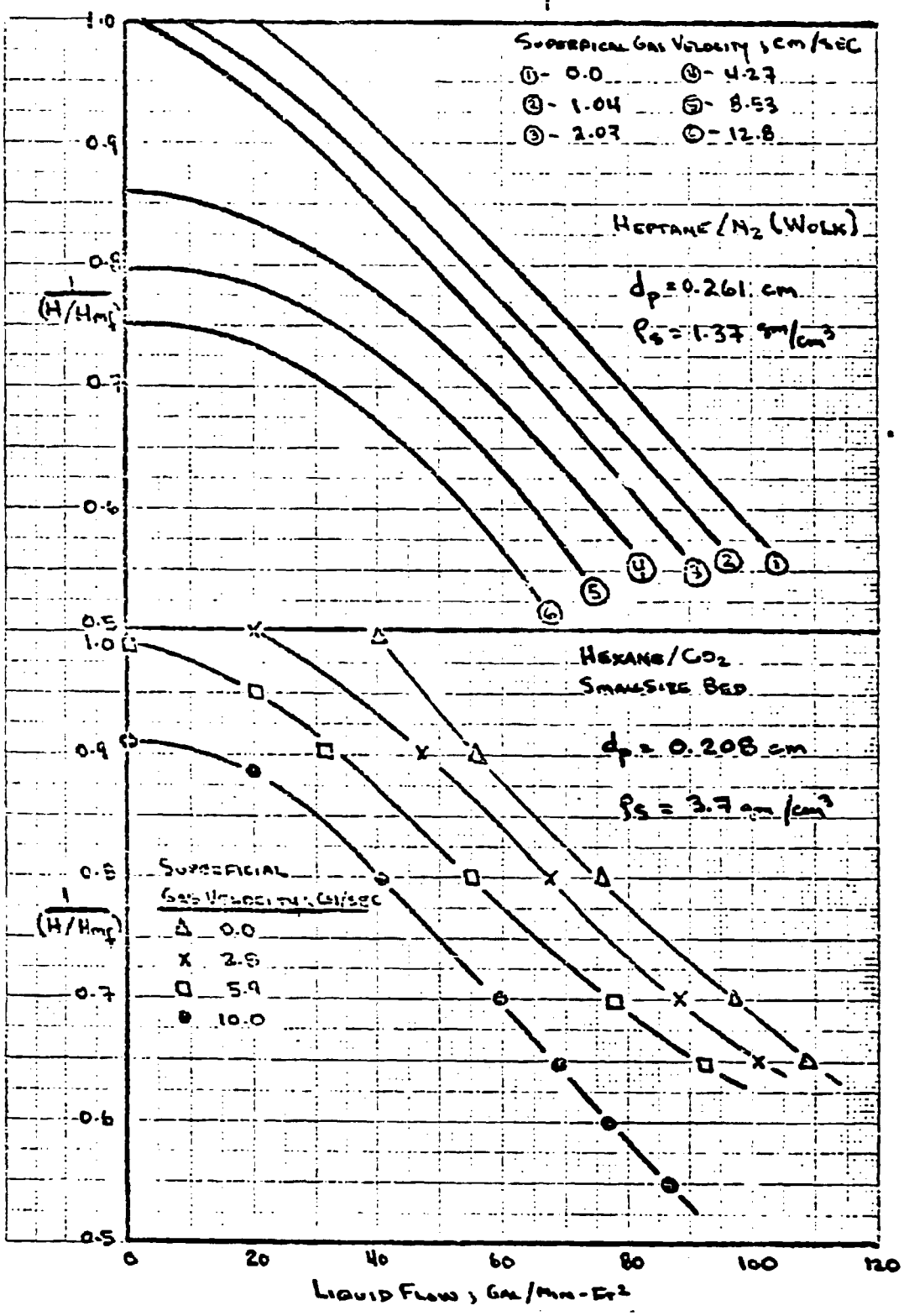

C. Conclusions

At superficial gas velocities less than 0.6 cm/sec, bed expansion ratios are independent of gas flow. Under these circumstances, results with a single fluid can be extended using the reduced superficial liquid velocity (with respect to the particle terminal velocity), to predict the behavior of the same fluid-solid system at other temperatures, or more important, to predict the bed behavior using fluids with different physical properties. Due to the low dependency of bed voidage upon gas velocity, bed voidage will be increased by only 8% over the no-gas level at the highest gas rates expected in the methanation reactor (equivalent to 2500 standard volumes of gas/hour - volume of reactor).

Direct application of the theoretical fluidization analyses to predict pressure drop, minimum fluidization velocity, etc. is not recommended since the predicted values are higher than the observed. As indicated before, this is due to varying particle geometry, wide particle size distribution, wall effects and temperature gradients. However, the experimental behavior on a relative scale is the same, as evidenced by the form of the fluidization and pressure drop curves and by our ability to correlate the data in a reduced form.

Most importantly, system pressure up to 1000 psig has no measurable effect on bed expansion behavior due to changes in gas density. In the future, this knowledge will enable us to accurately simulate, in a simple manner, the behavior of the high temperature - high pressure reaction systems by using a geometrically similar system at low pressure and low temperature. In retrospect, this result is understandable from the fact that at the relative liquid and gas flows encountered in our system, liquid flow is the dominant force in fluidization and if the effect of temperature on density and viscosity is considered, the fluidization at high temperature is identical to the behavior at ambient conditions. The effect of pressure and temperature on the gas phase is more difficult to predict but since this phase contributes very little to fluidization, predicting its behavior is not as essential.

V REVIEW AND DISCUSSION OF OTHER ASPECTS OF LIQUID-GAS-SOLID FLUIDIZATION

A. Heat and Mass Transfer

Gas and to a lesser extent, liquid fluidized beds have been employed in chemical engineering practice over a number of years. In many of the applications, the addition or removal of heat through the retaining wall of the bed is of major importance and in the case of gas fluidized beds has been the subject of extensive research. However, it is only in more recent years that a few reports have become available on the topic of heat transfer in liquid fluidized beds. Fluidized beds are desirable from a heat transfer point of view because of the high heat exchange rate which is attained in them. Mass transfer effects in fluidized beds have not received much attention until very recently. As in the case of heat transfer, an attractive characteristic of the fluid bed is its high rates of mass flux.

There are three pertinent modes of heat transfer; (1) convective heat transfer between points in the bed caused by mixing of particle and the homogeneous phase, (2) surface heat transfer between particles and fluid, and (3) transfer between the particles and the fluid and the walls of the vessel. The first two modes produce an effective heat conduction or diffusion in a fluidized bed while the third one provides the means to transfer heat to and from the outside of the fluidized vessel. These various modes of heat transfer are discussed below in more detail.

1. Heat Transfer in the Bulk Phase

In general, the basic difference between heat transfer within gas fluidized and liquid fluidized beds results from the relative solid-fluid heat capacities. In the gas bed, the incoming gas rapidly attains solid particle

temperatures within inches of the distributor because of the low heat capacity of the gas. In the liquid bed, however, heat transfer occurs, in most cases, throughout the entire bed. This is an important point to keep in mind when analyzing heat transfer and temperature profiles in fluidized beds.

In order to account for the presence of heat resistance throughout the bed, it is necessary to consider that the particles and the fluid are moving radially as well as axially. The radial movement of the liquid is due to density gradients and to wake movement associated with the motion of the particles. The heat transferred by such a mechanism would be a function of the particle concentration $(1-\epsilon)$ and the rapidity of particle motion as measured by particle Reynolds number.

Both of these contribute to a relationship of the form:

$$h = a\,(R_e)^z\,(1-\epsilon)^y \qquad (9)$$

which conforms to the experimental evidence.

2. Heat Transfer from Particles to the Bulk

Heat transfer from solid particles to fluid in fluidized beds is generally examined by extending the results for the single sphere heat transfer case [6] which can be represented by:

$$Nu_p = \frac{h_p d_p}{k_1} = 2 + 0.6\ Pr^{1/3}\ Re_p^{1/2} \qquad (10)$$

A first step in this extension would be the case for packed beds. Available data fit an identical form of equation 10 but the constant multiplier, 0.6, is replaced by 1.8 for Re_p greater than 100. The results for a fluidized bed, however, are not so clear. Over a thousand-fold variation exists among observers. This is a result of the variation

in experimental conditions (steady state or unsteady state) as well as the data interpretation of these investigators. In particular, their choice of assumed flow pattern (eg. plug flow or back mix) and also what thermocouple readings mean to each investigator (eg. for some, a bare thermocouple is taken to be the fluid temperature; for others, it is the solid temperature) have a strong influence of the experimentally measured heat transfer coefficient. All investigators agree in that there is a sharp drop in Nusselt number at particle Reynolds numbers less than 100; and for Reynolds numbers greater than 100, the Nusselt number is somewhere between the single sphere and packed bed case.

3. Heat Transfer from Wall to Bulk

Jogannadharaju & Rao [7] correlating existing data, found the following equation for wall-to-bed heat transfer.

$$J_H \epsilon = 0.53 \left(\frac{Re_p}{1-\epsilon} \right)^{-0.38} \qquad Re_p = \frac{\rho d_p \bar{u}}{\mu} \qquad (11)$$

This represented the data over a wide range of Prandtl numbers.

For glass spheres in water, Wasmund and Smith [8] found

$$\frac{1}{St_H} = \frac{Re_o^{1/3}}{10^{(0.11-1.75\epsilon)}} + \frac{\bar{u} D_i}{8 \left[1.06 \times 10^{-3} Re_o + 515 D_p (\epsilon - 0.5) \right]} \qquad (12)$$

where

St_H = Stanton Number at the Wall = $\frac{h}{C_p \rho \bar{u}}$

and

Re_o = The Particle Reynolds Number at the Particle Terminal Velocity = 1

Here though, the effects of process variables are somewhat obscure. A similar equation was obtained for aluminum particles.

All past researchers have observed that the heat transfer coefficient, h, varies with porosity, ϵ, in such a way as to give a maximum value, h_{max}, at a particular porosity. Both h_{max} and the corresponding porosity, ϵ_{max} are functions of the particle diameter, D_p. Increasing D_p results in an increased h_{max} and a slightly decreased ϵ_{max}. Hamilton [5] in view of the poor fit to the experimental data, reexamined the data of Wasmund and Smith [8] and Wasmund [9] by a Colburn factor approach.

$$J_H = \frac{Nu}{Re_p \, Pr^{1/3}} = K \left(\frac{Re_p}{1-\epsilon}\right)^{n-2} \qquad (13)$$

The relationship between bed expansion and Reynold's number determined by Richardson and Zaki [10] can be conveniently expressed by:

$$Re_p = Re_o \epsilon^m \qquad (14)$$

where Re_o = Particle Terminal Velocity Reynolds Number
ϵ = Porosity
m = Experimentally Determined Constant

Substituting equation 14 into equation 13 and rearranging gives:

$$Nu = Pr^{1/3} K Re_o^{n-1} \left[\epsilon^{m(n-1)} (1-\epsilon)^{2-n}\right] = K Pr^{1/3} Re_o^{n-1} \phi(\epsilon) \qquad (15)$$

where $\phi(\epsilon) = \epsilon^{m(n-1)} (1-\epsilon)^{2-n}$

After an additional dimensionless group, D_p/D_t, is introduced to account for the observed particle dependence, the resulting correlation was evaluated as:

$$Nu = 3.38 \left(\frac{D_p}{D_t}\right)^{.57} Pr^{1/3} Re_o^{0.565} \left[\epsilon^{0.565m} (1-\epsilon)^{0.435}\right] \qquad (16)$$

where the power dependence for the Prandtl number was assumed to be 1/3 to conform with the j-factor approach of Colburn[11].

Subsequent work by Brea and Hamilton[12] with heat transfer to a similar fluidized bed from a central heater, examined the effect of Prandtl numbers on the heat transfer coefficient, resulting in a modified form of equation 16.

$$\frac{h}{D_p k} = Nu = 0.943 \left(\frac{D_p}{D_h}\right)^{.15} Pr^{.52} Re_o^{.55} \left[\epsilon^{0.55m} (1-\epsilon)^{.45}\right] \qquad (17)$$

A physical interpretation of this heat transfer model is as follows. Increasing the particle size results in increased particle terminal velocity; thus an increase in the Reynolds number. There is an additional beneficial effect of having a bigger particle which is probably related to the decrease in film thickness with bigger particles. This effect is qualitatively given by the D_p/D_h ratio.

Bed porosity affects the heat transfer coefficient by again reducing film thickness with increasing porosities. This behavioral trend is reversed at a certain porosity level at which point further increases in bed porosity result in a decrease in heat transfer coefficient. This is explained on the basis of the detrimental effect of a reduced number of pellets when the porosity is very high.

4. Mass Transfer from Wall to Bulk

Mass transfer from a tube wall in a fluidized bed has been studied by two techniques: (1) dissolution mass transfer and (2) ionic mass transfer. Dissolution mass transfer experiments by King[13] utilized cylinders of cinnamic acid with glass spheres and water as the fluidizing medium. The measured mass transfer coefficients were found to be 5-10 times higher than the mass transfer coefficients in a tube without glass beads at equivalent tube Reynolds number. Unfortunately, in dissolution experiments a roughness pattern tends to develop which can be expected to lead to erroneous results, particularly at the very high Schmidt numbers encountered with dissolution mass transfer to a liquid. Brennan [14] has indicated that at a Schmidt

number of 2000, a roughness of 300 microinches increased the mass transfer almost seven times above that for a smooth surface. In the fluidized bed measurements of King[13], roughness measurements on the cinnamic acid cylinders gave values of about 100 microinches. Consequently, his data are open to question due to this effect.

The roughness effect which always seems to occur in dissolution mass transfer experiments is avoided when mass transfer data are generated via diffusion controlled reactions. The system that is particularly useful is the redox reaction between potassium ferrocyanide and potassium ferriccyanide in which there is no loss of diffusing species due to the reaction at the electrodes. This technique was used by Jottrand and Grunchard [14] to measure mass transfer coefficients for immersed nickel plates in liquid fluidized beds. The mass transfer coefficients were between five and ten times those measured in solid-free liquids at equivalent flow rates. As in the case of heat transfer, a maximum in the mass transfer coefficient was obtained at a porosity of 0.58, and the mass transfer coefficient increased with increasing particle size. The data could be represented by:

$$j_D = 0.027\, Re^{-0.375}\, Sc^{0.292}\, \frac{(1-\epsilon)^{0.15}}{\epsilon^{2.25}} \qquad (18)$$

Jogannadharaju and Rao [7] measuring ionic mass transfer coefficients in an annulus found their data could be correlated by a form similar to that used to represent their heat transfer results; the difference between these two expressions was that the constant 0.53 was replaced by 0.43.

$$j_D \epsilon = \frac{k_c \epsilon}{u} \left(\frac{\mu_l}{\rho_l \mathcal{D}}\right)^{2/3} = 0.43 \left(\frac{Re_p}{1-\epsilon}\right)^{-0.38} \qquad (19)$$

A continuation of the work of Rao by Krishna et al[15] showed that the central tube has the effect of reducing the outer wall mass transfer

coefficient. If a small wire is used as the inner electrode, mass transfer coefficients (equation 19) were increased by 50%. Consequently, the expression given above would predict a low mass transfer coefficient.

5. Mass Transfer from Particles to the Bulk

Similar to the work done on heat transfer from particles to fluid in a fluidized bed, dissolution mass transfer experiments are examined using the single sphere mass transfer case as a basis for comparison. The results for single sphere experiments are given by:[16]

$$Sh = \frac{k_d\, y_{LM} d_p}{\rho} = 2 + 0.6\, Sc^{1/3}\, Re^{1/2} \qquad (20)$$

Where y_{LM} Logarithmic mean fraction of inert or non-diffusing component.

Packed bed data could be represented by:

$$Sh = 2 + 1.8\, Sc^{1/3}\, Re_p^{1/2} \qquad Re_p > 80 \qquad (21)$$

while for fluidized beds, the data may be summarized by:

$$Sh = 2 + 1.5\, Sc^{1/3} \left[Re_p\, (1-\epsilon)\right]^{1/2} \qquad 5 < Re_p < 120,\ \epsilon \leq 0.84 \qquad (22)$$

Though no data exist for the low Reynolds number region, by analogy to the heat transfer solution, an expected sharp drop in mass transfer coefficients snould occur at Reynolds numbers less than 100.

Mass and Heat Transfer Analogy

Comparisons between the overall heat transfer coefficients (as j_H) and the overall mass transfer coefficients (as j_D) are inadequate when the Schmidt number is very much greater than the Prandtl number [17]. In heat transfer ($Pr \simeq 1\text{-}20$), the total resistance to heat transfer consists of a wall resistance, $1/h_w$, and a bed resistance, R_B, in series. In mass transfer, however, the large Schmidt numbers ($Sc \sim 1000$) preclude the existance of a bed resistance, and the resistance to mass transfer exists entirely at the wall. Only at higher Reynolds numbers, when the effect of the bed resistance is minimal, will the values of j_D and j_H be comparable.

B. Flow Benavior

1. Licuid-Solid Fluidized Beds

As an introduction to the more complex situation in three phase fluidization, some comments on the liquid-only fluidized bed are in order. Experiments utilizing colored tracer particles have been made to examine particle velocities in a three cylindrical coordinate system as a function of the superficial liquid velocity[18]. The results show tnat there is a linear relationship between the square of the individual velocity components, u_i, and the reduced fluidization velocity, u/u_{mf}.

$$u_i^2 = k_i \left(\frac{u}{u_{mf}} - 1\right) \qquad (23)$$

$i = z, r, \theta$

$u \geq u_{mf}$

u = Superficial Liquid Velocity

u_{mf} = Minimum Fluidization Velocity

The k_i are proportionality constants and are in the ratio:

$$k_z : k_\theta : k_r = 15 : 4 : 3$$

From tne values of the k_i, it is readily apparent that the velocity field is highly anisotropic, the low radial velocities occur mainly because of the restraining effects of the walls, and the high axial velocities occur because of the upward flow of the fluidizing medium. In addition, a well defined circulation pattern with particles rising in the center and moving downward at the walls, was evident. This circulation pattern is most noticeable at the bottom of the bed and tends to die out towards the top.

2. Liquid-Gas-Solid Fluidized Beds

a) Introduction

Flow studies on three phase fluidized beds have been limited to the study of bed expansion (examined in Section III-C) and bubble properties and mixing patterns. Rigby et al [19] examined a glass (sand) - air - water system and obtained data on bubble frequency, bubble size and size distribution, local volume occupied by gas bubbles and bubble velocity.

b) Bubble Properties

The bubble frequency measured as bubbles per second, shows a peak at low bed heights at between 0.4-0.75 times the radius. As you move up the column, this peak moves toward the center of the tube. Increasing the liquid rate or decreasing the bubble size results in a more uniform frequency distribution in the radial direction. This tendency for bubbles to move towards the center of the tube may necessitate the use of distributors which allow greater gas flows nearer the tube wall than at the tube center and thus redistribute bubbles uniformly in the radial direction.

For a given gas rate, the bubble size was found to decrease with increasing liquid rate. As expected, increasing height position in the bed results in an increase in bubble size. Decreasing gas rates also increase bubble size. This is caused by bubble coalescence which is a strong function of bed expansion.

Bubble velocity is a complex function of both liquid and gas flow rates. For a given bubble size, increased liquid or increased gas flow increases the bubble velocity. Also, there is a strong dependence on bed voidage as shown by the following correlation:

$$\left[V_B - (V_L + V_G)\right] \left[\frac{1-\epsilon}{\epsilon}\right]^2 = 32.5\ (1)^{1.53} \qquad (24)$$

where V_B, V_L and V_G are the bubble velocity and the superficial liquid and gas velocities in cm/sec, and l is the axial length of the mushroom-shaped bubble.

An additional consequence of the changes in bubble velocity is the effect of bubble velocity on gas holdup in the three phase fluidized bed. At low gas flow rates ($V_G < 1.0$ cm/sec), gas holdup is small, less than 5% by volume, and results chiefly from the quantity of bubbles present in the column as dictated by bubble frequency and rise velocity. At higher gas flows, however, the gas phase behaves as an additional force in bed expansion resulting in a steadily increasing gas holdup volume rising to values of 15% and 33% at gas velocities of 8.5 cm/sec and 25 cm/sec respectively. These increased gas holdups may have important consequences when considering both mass transfer rates from the gas phase to the liquid phase, and gas residence time for reaction.

c) Mixing Patterns

Mixing in a three phase fluidized bed has important implications, especially as it applies to reaction systems where the solid particle is a catalyst for the reactive gas and/or liquid phases. Here we are concerned with both temperature and concentration variation throughout the bed. Reman [20] has characterized axial mixing (back mixing) through a "mixing length". The mixing length is zero for ideal displacement and positive for all other cases.

Experiments by Vail et al [21] to determine mixing length in three phase fluidized beds have shown that while increased gas velocity increased axial mixing, increased liquid flow decreases axial mixing. Increasing the kinetic energy of the entering fluid (by decreasing flow area of the distributor) increases the axial mixing. For example, a four-fold increase in the jet velocity increases the mixing length by 30-40%. Most interesting was the observation that the presence of a solid phase reduces axial mixing from 50-70% over the no-solids case.

Radial mixing patterns followed the same trends observed with axial mixing lengths. Backmixing increases with increased gas flow and it decreases with increased liquid flow. Backmixing also increases with increased kinetic energy of both the gas and liquid phases.

C. Commercial Systems Using Liquid-Gas-Solid Fluidization

1. The Fischer-Tropsch Oil Circulation Process (22-24)

During the course of past development of the Fischer-Tropsch synthesis in Germany and in the United States, several processes, differing chiefly in the method of removing the heat of reaction, have been studied. These processes have been classified in the order of their development as follows:

a) Processes using fixed beds of granular or pelleted catalysts, cooled by indirect heat exchange, with and without recycle of the tail gas. Precise temperature control was difficult to maintain in the fixed bed system for it had been found in 1935 that most of the reaction took place in the middle of the catalyst bed and that most of the heat was liberated at that region.

b) Processes using fixed beds of granular or pelleted catalysts with internal cooling by direct heat exchange, such as the hot gas recycle and oil recycle processes.

c) Processes using suspensions of finely powdered catalysts in the liquid phase; the oil slurry and fluidized bed systems.

The third alternative is a homologous system of the liquid phase methanation scheme being investigated.

Development of the oil recycle process with a fixed, submerged catalyst bed was started in 1934 at the I. G. Farbenindustrie at Oppau. For several years pilot plants with converter volumes of 7 to 50 cubic feet were successfully operated by I. G. Farbenindustrie. However, because of World War II, the process never reached a commercial scale. The

initial work at the Bureau of Mines using oil as a coolant was begun with a flow of oil trickling downward over the catalyst. In a short time, it was found that smoother operation and better temperature control could be obtained by submerging the catalyst bed completely in the oil.

Fresh feed and recycle gas enter the bottom of the converter and flow upward concurrently with the circulating oil. As the gas passes over the catalyst, reaction occurs and heat is transferred to the cooling oil.

There are several fundamental differences in the fixed bed operation at the Bureau of Mines as compared to that of the German process. These are:

a) Use of a higher boiling cooling oil (300^{o} to 450^{o}C boiling range at atmospheric pressure) than that recommended and employed in Germany resulted in removal of the heat of reaction largely as sensible heat rather than by vaporization. This allowed more efficient recovery of the heat of reaction but, of more importance, it made the system pressure an independent variable.

b) Because most of the heat was removed as sensible heat in the recycle oil, a variation of the oil recycle rate made it possible to vary the temperature differential across the catalyst bed. Because the entire catalyst bed is at the most effective operating temperature, greater catalyst activity and durability are attained.

c) Use of a recycled tail gas, from which the water formed in the reaction had first been largely condensed, reduced the partial pressure of the water and affected the shift reaction as shown in the equation: $H_2 + CO_2 \rightleftharpoons H_2O + CO$.

Thus, by variation of the gas recycle rate, it was possible to change the hydrogen to carbon monoxide usage ratio (proportion of hydrogen to carbon monoxide consumed in the synthesis) of the synthesis gas within certain limits. The usage ratio could then be made more nearly equal to the hydrogen to carbon monoxide ratio in the feed gas and thus, more complete consumption of the synthesis gas was effected.

Both granular and pelleted precipitated iron catalysts were used in the initial experiments. These catalysts were active, but after relatively short periods of operation they crumbled or fused together, and inoperable conditions resulted.

A new method of operation - the moving catalyst bed - was developed to eliminate this cementation problem. Catalyst particles (10 to 40 mesh) were charged to the converter for moving bed operation, and the linear velocity of the cooling oil was increased to such a value that the catalyst bed expanded until the bed height was about 25 to 35% greater than its settled height. Considerable motion of the individual particles resulted from the high rate of oil circulation. A moving bed of synthetic ammonia-type catalyst was operated successfully in this manner for several months without any increase in the pressure drop across the catalyst and entirely without cementation of the bed. Although considerable attrition of the catalyst occurred, even after four months of operation, this had little or no effect on the activity, and the catalyst carry-over from the converter to the oil circulating lines was negligible. Other advantages of the moving bed as compared to the fixed bed are:

a) Greater catalyst economy is achieved by the use of smaller catalyst particles with greater geometric surface area per unit weight; this results in greater conversion per pound of catalyst at the same conditions of synthesis.

b) Lower operating temperatures are possible for the same amount of conversion.

c) Charging or withdrawing catalyst is facilitated both during operation or on termination of a run.

d) Since the pressure drop across the moving bed is almost independent of the rate of oil circulation (within the range of flows employed), less energy is required for a given temperature differential in the moving bed than for the same differential in the fixed bed.

e) A greater space-time yield based on converter volumes as well as catalyst volume is obtained.

The process has not been commercialized and it is doubtful that it will in the next decade. Their work, however, provides very useful information in gas-liquid-solid systems in which CO and H_2 are reacted to make hydrocarbon products.

2. H-Oil Process (25-26)

In the H-Oil process, a mixture of oil and hydrogen is fed upshot into an ebullating bed of catalyst. In the ebullating bed, the catalyst is expanded somewhat in excess of its settled volume and is in a state of motion induced by the velocity of the oil and hydrogen. Expansion and motion of the catalyst allows a wide latitude with respect to the effect of reactor geometry and catalyst size on reactor pressure drop, and avoids the limitations of the analogous fixed bed system by permitting fine solids to migrate through the bed and leave the reaction system. The motion of the catalyst together with the high velocity of oil in the system also results in intimate contact between oil, hydrogen, and

catalyst, making the reaction system very efficient with respect to the amount of catalyst charged per unit of oil throughput. Catalyst attrition is insignificant, since the particles in motion in the ebullating bed are cushioned by an envelope of oil. Furthermore, the catalyst is retained within the volume of the reactor so that it is completely unnecessary to provide means for separation from the product oil and recharging to the system.

An important advantage of the ebullating bed is that it allows catalyst to be added and withdrawn from the reactor system semi-continuously.

A second feature of the H-Oil process is internal recycle. Liquid oil, in equilibrium at reactor outlet conditions, is pumped back to the inlet and again passed through the reactor. This internal recycle creates a sink into which the large amounts of heat produced in the process are dissipated. The amount of recycle used depends mainly on the amount of heat evolved.

As it can be seen, the H-Oil process is another homologue of the liquid phase methanation system being investigated. As in the latter, the former reacts a gas in the presence of a liquid and a solid catalyst. This process has been commercialized and in one small unit in Louisiana and another in Kuwait, these operated very satisfactorily for a number of years. A third larger unit was built at Humble Oil's Bayway Refinery in New Jersey. After a year of operation, an explosion occurred and caused considerable damage to the reaction section. Humble has not indicated the reasons for this mishap but there are indications that the explosion took place because of an operational error.

The basic reason for reviewing these two processing schemes is to put our work on liquid phase methanation within the framework of the technology on liquid-gas reactions catalyzed by a solid. In addition to the two processes included herein, it should be kept in mind that

there are numerous chemical syntheses in which a liquid is reacted with a gas in the presence of a solid catalyst. Among these are various hydrogenation reactions and a few hydrocarbon oxidations. They are not discussed in any detail herein mainly because the processing scale is much smaller than the one envisioned for the methanation reaction.

The relevance of the Fischer-Tropsch and the H-Oil systems is largely related to their similarity in scale which indicates that numerous common problems will exist. The knowhow derived from the above mentioned processes will be extremely valuable in the development stage of the liquid phase methanation system.

VI REVIEW OF THE COMMERCIAL METHANATION PROCESSES

Methanation of CO and H_2 has been widely practiced for a number of decades. In most cases, this process was part of the hydrogen plants in which methane was reformed with steam into CO_2 and H_2. The small amounts of CO generated during the reforming stage were reconverted back to methane in a fixed bed reactor.

With the advent of coal gasification first in Europe and at a later date in the United States, methanation of gas streams containing higher concentrations of CO and H_2 became a necessity. The crucial problem inherent in the methanation step is the large amount of heat evolved by the reaction which required complicated and expensive schemes to remove the heat. In essence, most of the work done in this area has been directed towards the method to remove the heat of the reaction.

Prior to a brief review on the commercial process, it seems desirable to discuss both the reaction itself and the catalysts employed for that purpose.

A. Kinetic Studies

The basic reaction is given below.

$$CO + 3H_2 \rightleftharpoons CH_4 + H_2O$$

There are other potential reaction paths which are represented by the following equations:

$$CO + H_2O \rightleftharpoons CO_2 + H_2$$

$$CO + H_2 \rightleftharpoons C + H_2O$$

In most cases, these two reactions are insignificant but they can become important if the temperature is above 350°C.

As expected, a very substantial amount of work has been done with feeds containing very small amounts of CO and H_2. A number of catalyst systems including nickel, ruthenium, rhodium, palladium and platinum have been investigated [27]. These studies do not have as much value as the work done with high concentration feeds [28-31].

All authors agree that the rate of methane formation is proportional to the partial pressure of CO. The hydrogen concentration effect of the rate is a source of disagreement since some authors propose a rate expression strongly influenced by hydrogen partial pressure while others indicate that the rate is only mildly affected by hydrogen partial pressure. To a large extent, the differences have arisen from studying the reaction under widely varied reaction conditions; such as temperature, pressure and feed composition.

A point that should be made is that regardless of the actual exponent of the hydrogen partial pressure term in the equation, all the rate expressions take the form of Langmuir-Hinshelwood kinetics in which adsorption on the catalyst surface is a controlling step in the reaction. This must be kept in mind when evaluating the data generated in the presence of a liquid phase.

B. Catalyst Systems

Most commercial methanation catalysts are nickel based. The kinetic data briefly reviewed above were generated with nickel catalyst supported either on Kieselguhr or on silica. In some cases the nickel metal was used as the catalyst without a support.

Other metals, notably those in the noble metal family, are capable of catalyzing the methanation reaction. The results, however, have not proven to be sufficiently good as to warrant its commercial use namely because of their very high cost.

In the liquid phase methanation study, it is planned to use commercial methanation catalysts provided by manufacturers such as Girdler, Harshaw and Catalyst and Chemicals. All of these are nickel based catalysts on a support whose difference is limited to size and nickel loading.

C. Commercial Processes

As indicated before, most commercially available processes use a nickel based catalyst and their process differences are essentially in the method used to remove the reaction heat and the reactor configuration.

Among the various alternatives proposed as solutions to the heat removal problem are (1) introduction of cold feed gas at different points in the reactor train, (2) recycle of large quantities of product gas, (3) gas-solid fluidized bed reactors and (4) tube wall reactors where the catalyst is bonded to the tube wall.

Conceptual designs for gas methanation use fixed bed adiabatic reactor systems which are cooled directly by gas recycle or cooling of the feed gas between stages [32] [33] [34] to control the heat release. The designs use nickel-alumina catalysts which, although sensitive to sulfur compounds, are highly active and permit high space rates of 5000-10,000 SCF/cubic foot to be achieved. (The removal of sulfur compounds from the gas, in any event, is a necessary step either before or after methanation because of the specification of less than 0.25 grains of sulfur per 100 cubic feet for pipeline gas.) Techniques for lowering the sulfur in gases to such low levels are available.

The Institute of Gas Technology investigated fixed bed systems using complex Dowtherm heat exchange equipment in the catalyst trays that served to cool the gas indirectly. The work was abandoned and it was concluded that such an approach was impractical for the design of large scale, fixed bed reactors for essentially complete conversion of synthetic gas to methane[35].

Gas-solid fluidized bed reaction systems for methanation in pilot plants have been carried out by the Bureau of Mines and the Institute of Gas Technology. Fluidized beds feature the usual high rates of heat transfer and the ease of addition and withdrawal of catalyst as an additional advantage. However, restrictions of the possible range of operating conditions (the solid could be fluidized over a relatively narrow velocity range), back mixing effects, and attrition of the catalyst were recognized as problems, as was scale-up to commercial plant size [36] [37].

The Institute of Gas Technology's pilot plant work suffered from losses of catalyst from the bed and coking of a portion of the catalyst which resulted in a decreased synthesis gas conversion capacity [35]. Reportedly, gas-solid fluid bed work on methanation is continuing at Bituminous Coal Research's laboratories.

Because of the difficulty of removing the heat of reaction, the Bureau of Mines has performed pilot plant work with Raney nickel catalysts that are bonded to the outer surface of metal heat exchanger tubes. Boiling Dowtherm in an annular space takes up the heat of reaction. The Bureau's work [31] [38] [39] has been encouraging in that yields of up to 300,000 SCF of high BTU gas per pound of catalyst have been achieved, although some difficulties were encountered in the experimental work with flaking of the catalyst from the walls due to formation of nickel carbide. Some erratic results were also experienced in scaling up from bench scale tests in that methanation results in the pilot unit were performed at a feed rate of 54 SCF per hour per square foot of catalyst as compared to 105 SCF per hour per square foot of catalyst surface in earlier Bureau of Mines' test work. (The Bureau's overall gas space velocity, ca 500 to 600 SCF/CF reactor space, seems to offer no apparent advantage over fixed bed space rates.)

Economic evaluations of all the various processing alternatives have indicated that the methanation step is a relatively expensive step. The difference in the economics of the product recycle case and the inter-reactor quench case are relatively small and consequently in the section

below, the recycle case economics are summarized. Fluid bed economics are not presented herein in any detail but clearly a noticeable decrease in reactor cost will result if this process scheme is commercialized.

The capital and operating costs for a 250 MM SCFD plant are summarized in Table VI-1. As it can be seen, the plant requires a substantial expenditure of capital and its operating costs are quite substantial since they amount to close to 4c/MSCF. This figure excludes the cost of the feedstock and only represents the cost of upgrading the synthesis gas to methane. In addition, the return of the capital invested has not been considered but even at the low level of 10% return before taxes, this would represent an additional 1.5c/MSCF.

The economic advantages of a liquid phase methanation system are related to both capital and operating cost. As in the case of the gas fluidized system, the reactor costs are going to be less due to the greater simplicity of construction of a tube-free reactor. An additional advantage of the liquid fluidized system is that heat removal becomes substantially more efficient and a noticeable decrease in heat exchanger surface will be attained. By using a concentrated feed; one containing up to 20% CO and 60 H_2: the productivity volume of equipment is going to be substantially increased This will be reflected mainly on the power costs which, as indicated in Table VI-1, are very substantial in a fixed bed process plant.

TABLE VI-1

Fixed Bed Methanation - Economic Analysis
250 MM SCFD Plant

Process	Fixed Bed
Category of Cost	
Reactors	$ 1,800,000
Exchangers, Heaters	1,140,000
Compressors and Pumps	1,164,000
Knockout Drum	348,000
Instruments, Controls, and Valves	2,775,000
Total Cost of Equipment	7,227,000
Engineering	500,000
Construction	4,000,000
Plant Cost	11,727,000
Contractor's Fee at 5%	586,300
Interest During Construction at 5%	615,600
TOTAL	$12,928,900

Production Costs

	Rate	Unit Cost	$/Year
Steam	7,000,000 MM BTU	40¢/MM BTU	(2,800,000)
Power	20,000,000 KWH	1¢/KWH	2,000,000
Cooling Water	10,000,000 M Gals.	2.5¢/M Gal.	250,000
Labor	2 Man/Shift*	$9,000/Year	72,000
Catalyst			400,000
Overhead Expenses**			2,570,000
TOTAL COST OF PRODUCTION			$2,492,000

* Total Manpower = 8 Men

**Assumed to be 20% of Capital Cost

VII DEVELOPMENT OF ANALYTICAL SYSTEM

A. Analyses Required

The design of the analytical system is based on the following reactions:

$$3H_2 + CO \longrightarrow CH_4 + H_2O$$

$$2\ CO \longrightarrow C + CO_2$$

$$CO + H_2O \longrightarrow H_2 + CO_2$$

One analytical system will be constructed to separate and quantify CO, CO_2, CH_4 and other light hydrocarbons and will also identify trace amounts of air if present. A second system will be utilized to quantify H_2. H_2O will be quantified by means of H_2, C and O_2 balancing. Standard molecular sieve, carbosieve and silica gel packings and thermal conductivity detectors will be used to obtain the necessary separations and quantitation.

Initially all injections of samples will be made manually by means of gas sampling valves connected to the feed and effluent lines. These valves can be remotely actuated at fixed intervals during continuous reactor operation.

Initially quantitation of all components will be achieved by comparison of peak heights obtained on a 1 mv recorder to a plot of those obtained from injection of known quantities of standards. Continuous reactor operation will require the incorporation of an electronic integrator into the analytical system.

The following schematic illustrates the initial analytical procedure:

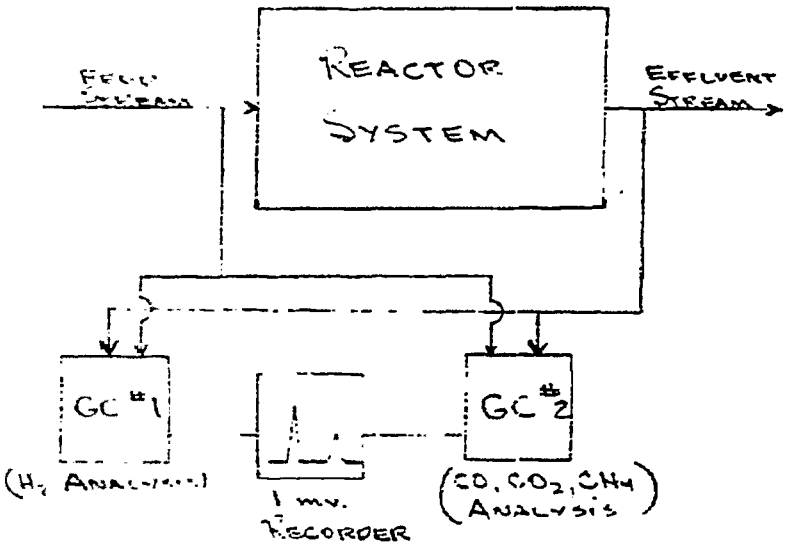

B. Available Equipment and Performance Ratings

There are numerous manufacturers who can supply the necessary equipment. It is assumed, by prior experience, that the purchased equipment will function reliably for the duration of the work and will be compatible with any electronic or mechanical additions which may be made in the future (remote sample valve actuators, electronic integrators. etc.).

C. Cost and Quotations

The necessary equipment for the initial analytical work ranges in price from $1800 to $2100. This includes two gas chromatographs equipped with sampling valves and columns. Quotations from three suppliers are attached. The equipment sold by Carle Instruments Inc. is best suited for all analytical work related to this reaction and is the only one in which the sampling valves can be operated remotely by later addition of a timer controlled actuator.

BIBLIOGRAPHY

1. Liquid Phase Methanation, Progress Report No. 1, Thermal Stability Study, Chem Systems Inc., June 1, 1972
2. Dakshinamurty, P., Subrahmanyan, V., and Rao, J. N., IEC Proc. Dev., 10(3), 322, 1971
3. Wolk, P., Ph.D. Thesis, Brooklyn Polytechnic Institute, 1962
4. Kunii, D. and Levenspiel, O., Fluidization Engineering, p. 77, Figure 5, J. Wiley and Sons, 1969
5. Hamilton, W., Can. Journal of Chem. Eng., 48 (Feb.), 52, 1970
6. Kunii, D. and Levenspiel, O., Fluidization Engineering, p. 210, J. Wiley and Sons, 1969
7. Jogannadharaju, G. J. V., and Rao, C. V., Indian Journal of Technology, 3, 201, 1965
8. Wasmund, B., and Smith, J. W., Can. Journal of Chem. Eng., 45, 156, 1967
9. Wasmund, B., Ph.D. Thesis, University of Toronto, 1966
10. Richardson, J. F., and Zaki, W. N., Trans. Institute of Chem. Eng. (London), 32, 35, 1954
11. Colburn, A. P., Tran. AIChE, 29, 174, 1933
12. Brea, F. M., and Hamilton, W., Trans. Institute of Chem. Eng. (London), 49, 196, 1971
13. King, D. H., B.A. Sc. Thesis, University of Toronto, 1965
14. Jottrand, R., and Grunchard, F., Proc. Symp., Interaction Between Fluids and Particles, London, 211, 1962
15. Krishna, M. S., Jogannaharaju, G. J. V., and Rao, C. V., Indian Institute of Technology, 4, 8, 1966
16. Kunii, D., and Levenspiel, O., Fluidization Engineering, p. 195, J. Wiley and Sons, 1969
17. King, D. H., and Smith, J. W., Can. Journal of Chem. Eng., 45, 329, 1967
18. Carlos, C. R., and Richardson, J. F., Chem. Eng. Sci., 23(8-A), 813, 1968
19. Rigby, G. R., VanBrockland, G. P., Parks, W. H., and Capes, C. E., Chem. Eng. Sci., 25, 1729, 1970

20. Reman, G. H., Chem. Ind. (London), 15(3), 218, 1952
21. Vail, Y. K., Manakov, N. K., and Manshilin, V. V., Int. Chem. Eng., 8(3), 516, 1968
22. U. S. Bureau of Mines Bulletin 568, Development of the Fischer-Tropsch Oil Recycle Process, 1957
23. Crowell, J. H., Benson, H. E., Field, J. H., and Storch, H. H., IEC, 42(11), 2376. 1950
24. Benson, H. E., Field, J. H., Bienstock, D., and Storch, H. H., IEC, 46(11), 2278. 1954
25. Chervenak, M. C., Johnson, C. A., and Schuman, S. C., Pet. Refinery, 151, October 1960
26. Schuman, S. C., CEP, 57(12), 49, 1961
27. Rehmat, A., and Randhava, S. S., IEC Prod. Res. Devel., 9(4), 512, 1970
28. Lee, A. L., Felkirchner, H. L., and Tajbl, D. G., ACS Paper
29. Akers, W. W., and White, R. R., CEP, 44(7), 553, 1948
30. Schultz, J. F., Karn, F. S., and Anderson, R. B., U. S. Department of Interior Report No. 6941
31. Haynes, W. P., Elliott, J. J., Youngblood, A. J., and Forney, A. J., Symp. on Hydrogen Processing of Solid and Liquid Fuels, Chicago, Illinois, ACS Meeting, Div. of Fuel Chem., September 13-18, 1970
32. C. L. Tsaros, et al., Process Design and Cost Estimate for Production of 266 Million SCF/Day of Pipeline Gas by the Hydrogasification of Bituminious Coal Inst. of Gas. Tech., August, 1966, Office of Coal Research Report, R & D Report No. 22
33. ANON., Engineering Study and Technical Evaluation of BCR "Two Stage Superpressure Gasification Process" Prepared for Office of Coal Research by Air Products and Chemicals Inc.
34. C. L. Tsaros, et al., "Cost Estimate of a 500 Billion BTU/Day Pipeline Gas Plant via Hydrogasification and Electrothermal Gasification of Lignite, Inst. of Gas. Tech. Report for Office of Coal Research, R & D Report No. 22
35. H. R. Linden, Conversion of Solid Fuels to High - Heating Value Pipeline Gas, AIChE Symp. on Hydrocarbons from Oil, Shale, Oil Sands and Coal, CEP, Symp. Ser., Vol. 61, No. 54, pp. 76-103 (1965)

36. Hall, C. C., Taylor, A., J. Inst. Petrol., 41, 101-24, 1955
37. Schlesinger, M. D., et al., Ind. Eng. Chem., Vol. 45, No. 2, 68-70, (1953), U. S. Bureau of Mines R. I. 5137 (1955)
38. Gilkeson, M., et al., Synthesis of Methane by Hydrogenation of Carbon Monoxide in a Tubular Reactor, IEC, Vol. 45, No. 2, Feb. 1953, p. 460-467
39. Field, J., and Furney, A., High BTU Gas via Fluid Bed Gasification of Caking Coal and Catalytic Methanation, AGA Proc. of Synthetic Pipeline Gas Symposium, 1966, p. 83-94

CSI-MPR--3

Chem Systems Inc.

LIQUID PHASE METHANATION

Progress Report No. 3

Table Of Contents

1. SUMMARY

For the month of July work on the methanation project focused mainly on completion and testing of the new methanation unit. Improvements in the analytical system are currently underway. These include (1) a more sensitive hydrogen analysis, and (2) hot product sampling for water vapor determination. Ultimately, the analysis will be performed with signal integration for peak area, rather than the present peak height method.

As per our discussions with the AGA representatives, we have calculated pertinent mass transfer rates, e.g., mass transfer from the gas interface to the bulk liquid, and diffusion of the reacting components from the bulk liquid to the catalyst surface, and found them to be more than on order of magnitude greater than the reaction gas feed rate. The values, at a 50% conversion level, are shown in the table below for two liquid systems; a paraffin oil and pseudocumene. The composition was assumed to be 25% CO and 75% H_2.

	Rate; gm moles CO / per hour	
	Liquid Phase	
	Paraffin Oil	Pseudo Cumene
Reaction Rate for a Flow Rate of 500 VHSV	2.2	2.2
Diffusion from Bulk Liquid to Catalyst Surface	64	350
Mass Transfer from Gas Interface to Bulk Liquid	22	70

In addition, thermodynamic equilibrium calculations were also performed, and show that aside from the main reaction to produce methane, the shift reaction occurs to a small, but measurable extent. The equilibrium compositions at 320°C and 72.45 atm. are:

Component	CO_2	CO	H_2	H_2O	CH_4
Mole Fraction	.00249	.0001	.00995	.493	.495

Further calculations indicate that at these conditions, carbon formation is negligible.

In putting the methanation on stream, several reaction runs were obtained. At the proposed gas flow rate of 500 SCF, volumes of gas/volume of reactor-hr, and a temperature of 320°C a CO conversion of 85% was obtained. Conversion levels based on H_2 and CH_4 were 60% and 65%, respectively. Discrepancies are probably due to non-equilibrium concentrations in the liquid and gas phases, and to the shift reaction which converts CO to CO_2.

II. COMPARISON OF REACTION RATES AND MASS TRANSFER RATES

At the proposed reaction conditions we are passing 500 standard volumes of gas per hour per volume of reactor. For the 400 cm^3 reactor this is equivalent to 50 liters/hour of CO and 150 leters/hour of H_2, and total conversion to CH_4 would require a value 2.2 gm moles CO reacted/hour. In order to determine, if under the proposed reaction conditions, whether or not conversion would be limited by some mass transfer mechanism (e.g., diffusion of the dissolved gases to the catalyst surface, or mass transfer from the gas interface into the bulk liquid), we calculated these mass transfer rates considering CO as the limiting reactant and either a paraffin oil or pseudo cumene as the fluidizing liquid.

1. Diffusion of CO From the Bulk Liquid to the Catalyst Surface

The overall rate of diffusion of CO from the bulk liquid to the catalyst surface can be represented by

$$N = k_c (C_l - C_s) \quad \frac{\text{gm moles}}{\text{sec-cm}^2}$$

k_c: mass transfer coefficient; cm/sec

C_l, C_s: concentration in the liquid and at the solid surface; gm moles/cm^3

Values for the mass transfer coefficients in small particle fluidized beds can be estimated from the relationship of Brian and Hales[1];

$$\frac{k_c d_p}{D}^2 = 4 + 1.21 \left(\frac{d_p U_l}{D}\right)^{2/3}$$

d_p : particle diameter; cm

U_l : liquid velocity; cm/sec

D: diffusion coefficient; cm^2/sec

where the diffusion coefficient can be predicted with the equation of Wilke and Chang[2]:

$$D = 7.4 \times 10^{-10} \frac{T (XM_2)^{1/2}}{\mu_l V_b^{0.6}}$$

T: absolute temperature; °K

X: empirical association parameter

M_2: solvent molecular weight

μ_l: solution viscosity; poise

V_b: solute molar volume determined from Kopp's Law; cm^3/gm mole

For CO, Kopp's Law gives erroneous results, and a value of 30.7 for V_b is preferred. The solvent properties at 573°K, tabulated below,

TABLE I

Solvent	M_2	X	μ
paraffin oil	420	1	0.0044
pseudo cumene	120	1	0.00044

and lead to diffusion coefficients for CO in the paraffin oil and pseudo cumene of 2.5 (10^{-4}) cm^2 and 13.2 (10^{-4}) cm^2/sec.

Combining this with a particle diameter of 0.045 cm and a normal liquid velocity of 1.0 cm/sec the calculated mass transfer coefficients are 3.46 (10^{-2}) cm/sec for the paraffin oil and 12.2 (10^{-2}) cm/sec for pseudo cumene. The catalyst surface concentration was taken to be zero and the bulk liquid gas concentrations (at a conversion of 50%) were obtained from Henry's Law coefficients, H: atm/mole fraction, determined by the method of Osburn and Markovic[3]. Briefly, this procedure involves estimating the Ostwald coefficient, L; cm^3 gas/cm^3 liquid, from the liquid surface tension, σ; dynes/cm. Unknown surface tensions may be estimated, using the Sygden parachor, [P], and the liquid density, ρ; gms/cm^3, from the relationship

$$\sigma = \frac{[P]\,\rho}{M_2}^4$$

For dilute solutions, the Ostwald coefficient is related to the Henry's Law constant by

$$H = \frac{1}{\frac{L}{22,400}\left(\frac{M_2}{\rho}\right)}$$

Hence by definition

$$H = \frac{pa}{\chi a} \quad \text{or} \quad \chi a = \frac{pa}{H}$$

where pa is the gas partial pressure in atmospheres and χ_a is the gas mole fraction in the liquid phase, the bulk liquid concentration can be approximated by

$$C_l = \frac{a}{(M_2/\rho)}$$

For our system, at a 50% conversion level, the CO partial pressure is 12 atmospheres and the calculations, reviewed in Table II result in CO concentrations in the bulk liquid of 5.1 (10^{-5}) gm moles/cm^3 for paraffin oil and 8.0 (10^{-5}) gm moles/cm^3 for pseudo cumene.

Solvent	M_2	ρ	σ	L	H	χ_A	$C_A \times 10^5$
paraffin oil	420	.865	40.5	0.095	483.	.025	5.1
pseudo cumene	120	.88	32.4	0.150	1095.	.011	8.0

Combining these liquid phase concentrations for the gas and the previously calculated mass transfer coefficients, we get mass transfer rates of 0.0064 $\frac{\text{gm moles CO}}{\text{hr-cm}^2\text{ catalyst}}$ (paraffin) and 0.035 $\frac{\text{gm moles CO}}{\text{hr-cm}^2\text{ catalyst}}$ (pseudo cumene). For our catalyst system and liquid flow rates there is about 50 $\frac{\text{cm}^2\text{ catalyst}}{\text{cm}^3\text{ expanded bed}}$, and further, since there is a minimum of 200 cm^3 of expanded bed the gross CO mass transfer rates are over 64 $\frac{\text{gm moles}}{\text{hour}}$ in paraffin oil and over 350 $\frac{\text{gm moles}}{\text{hour}}$ in pseudo cumene. These values are well over an order of magnitude greater than our CO feed rates of 2.2 $\frac{\text{gm moles}}{\text{hour}}$, and mass transfer by the mechanism will not be limiting.

2. Mass Transfer From the Gas Interface to the Bulk Liquid

Mass transfer limitations may also arise from transfer of CO from the gas phase to the bulk liquid. For swarms of small bubbles (<2.5 mm), mass transfer coefficients from the gas interface to the liquid are correlated by the same relationship that applies for small solid spheres. However, in deep vessels which are not mechanically agitated and with liquid viscosities of about 1 cl, the bubble diameters are on the order of 0.3-0.6 cm. Gas holdup is less than 20% and the interfacial area is estimated to be 1-3 cm^2/cm^3 of expanded bed. Under these circumstances, the mass transfer coefficient may be obtained from

$$k_l = \frac{0.42}{\left(\frac{\mu_l}{\rho_l D}\right)^{1/2}} \left[\frac{\mu_l g (\rho_l - \rho_a)}{\rho_l^2}\right]^{1/3}$$

k_l: mass transfer coefficient; cm/sec.

μ_l: liquid viscosity; poise

ρ_l, ρ_a: liquid or gas density; gm/cm^3

D: diffusion coefficient; $cm^2/sec.$

For our two liquids the calculated values are 0.147 cm/sec. for the paraffin oil and 0.482 cm/sec for the pseudo cumene. At the 50% conversion level, CO concentration in the gas phase is about $2.5(10^{-4})$ gm moles/cm^3. Combining this with the previously calculated liquid concentrations yields values for the gross CO mass transfer rates from the gas to the liquid of over 22 gm moles/hour in paraffin oil and over 70 gm moles/hour in pseudo cumene. Again these values are at least an order of magnitude greater than the feed rate of 2.2 gm moles CO/hour.

III. EQUILIBRIUM THERMODYNAMIC CALCULATIONS

Not only are we concerned with mass transfer limitations, but we must also recognize the possibility of an unfavorable equilibrium situation. We therefore performed equilibrium calculations for the system of reactors.

1. $CO + 3H_2 \rightleftharpoons CH_4 + H_2O$
2. $CO + H_2O \rightleftharpoons CO_2 + H_2$
3. $2CO \rightleftharpoons CO_2 + C$

For mathematical tractability, other forms of the reaction equations are preferred, these are:

4. $C + H_2O \overset{K_1}{\rightleftharpoons} CO + H_2 \qquad K_1 = \dfrac{[CO]\,[H_2]}{[H_2O]}$
5. $CO + H_2O \overset{K_2}{\rightleftharpoons} CO_2 + H_2 \qquad K_2 = \dfrac{[CO_2]\,(H_2)}{[CO]\,[H_2O]}$
6. $C + 2H_2 \overset{K_3}{\rightleftharpoons} CH_4 \qquad K_3 = \dfrac{[CH_4]}{[H_2]^2}$

The phase rule for chemical reaction can be expressed as

$$V = (N-R-ST) - P + 2$$

where V = variance of the system
N = species
R = chemical reactions
ST = storchrometirc relations
P = number of phases

For our system

$N = 6$
$R = 3$
$P = 2$
$ST = \dfrac{\text{moles H atoms}}{\text{moles O atoms}} = 6$

As a result, the variance of our system is 2, that is only temperatures and pressure can be varied independently. A computer program for solving the gas phase concentrations at equilibrium utilizes the 3 equilibrium equations, the stoichrometric relation and the additional constraint that the sum of the mole factions in the gas phase is equal to 1.0.

The initial results were essentially constant over a temperature range of 280-370°C and a pressure range of 20-80 atmospheres, and could be represented by the following solution for a temperature of 320°C and a pressure of 72.45 atm.

Component	CO_2	CO	H_2	H_2O	CH_4
Mole Fraction	.0497	.0001	.0076	.4359	.5067

However, subsequent examination of the results, e.g., the hydrogen to oxygen ratio is only 5.44 and not the 6.0 required by stoichiometry, shows that the solution has not truly converged. We feel this is due to a combination of (1) the criteria for convergence, and (2) the low concentrations of two of the components. Further work in the area is required. An alternative procedure for the solution to this reaction system is to consider only the following equations,

7. $CO + 3H_2 \rightleftharpoons CH_4 + H_2O$

8. $CO + H_2O \rightleftharpoons CO_2 + H_2$

and by solving for the predicted equilibrium values check to see if carbon would be formed via either of the two reactions.

9. $CH_4 \longrightarrow C + 2H_2$, or

10. $CO + H_2 \longrightarrow C + H_2O$

Preliminary calculations gave the following results

Component	CO_2	CO	H_2	H_2O	CH_4
Mole Fraction	.00249	< .0001	.00995	.493	.495

With these concentrations we can show that carbon would not form as a result of reaction 9. The CO concentration is too low to accurately calculate values for reaction 10, without the aid of a computer, through it looks as if there is sufficient water vapor present to preclude carbon formation via this reaction.

IV. EXPERIMENTAL RESULTS

During this month the unit was put on stream for some preliminary runs in order to study temperature profiles in the system as well as establish a standard operating procedure. The reactor was loaded with 193.5 gm of Girdler catalyst G65-RS which had been ground to a 30-50 mesh and treated with H_2 for 18 hours at 650°F. The dry volume of the catalyst was 210 cm^3 which is somewhat greater than one-half the reactor volume. The differential pressure cell and the high pressure rotameter were not yet installed and no water analysis was available at the time of the runs. In addition, an indeterminant amount of water vapor product condensed before sampling so it was not possible to get an accurate mass balance. The results for these few runs are tabulated below:

Run	Pressure	Temp.	Liquid Flow	Exit Gas Flow	Inlet Gas CO	Inlet Gas H_2	Outlet Gas CO	Outlet Gas H_2	Outlet Gas CO_2	Outlet Gas CH_4
1	800 psig	320°C	10 liter/hr.	115 liter/hr.	25%	75%	11%	50%.	1.5%	21%
2	800	320	20	105	25	75	7.7	48.5	3.4	28.0
3	800	320	20	230	25	75	15.7	58.0	1.6	11.0

For example the results for run #2 are equivalent to about 85% conversion of CO. 60% conversion of an H_2 and 65% conversion to an CH_4. The discrepancies arise from the fact that the shift reaction converts CO to CO_2 and that the system liquid, and gas phase concentrations may not have equilibriated.

Note the trend of the results - increased liquid flow (increased bed expansion and residence time) and decreased gas flow - both increase conversion levels. This is expected from an increase in bed expansion and residence time.

During the coming month, the experimental unit will be fitted with the differential pressure meter and a high pressure rotometer. The catalyst-liquid seam, described a previous summary report will be initiated during this month too.

V. BIBLIOGRAPHY

1. Brian, P.L.T., and Hales, H.B., AIChE J, 15, 419 (1969)

2. Wilke, C.R., and Chang, P., AIChE J, 1, 264 (1955)

3. Osburn, J.O., and Markovic, P.L., Chem. Eng., 108, Aug. 25, 1969

CSI-MPR--4

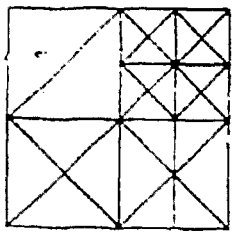

LIQUID PHASE METHANATION

PROGRESS REPORT #4

Prepared By Chem Systems Inc.
For the American Gas Association
August, 1972